Schweizerische Eidgenossenschaft
Confédération suisse
Confederazione Svizzera
Confederaziun svizra

Federal Department of the Environment,
Transport, Energy and Communications DETEC

Swiss Federal Office of Energy
Energy Research and Cleantech

Final report from 15 August 2025

TESK

Development of textile-based luminescent solar concentrators

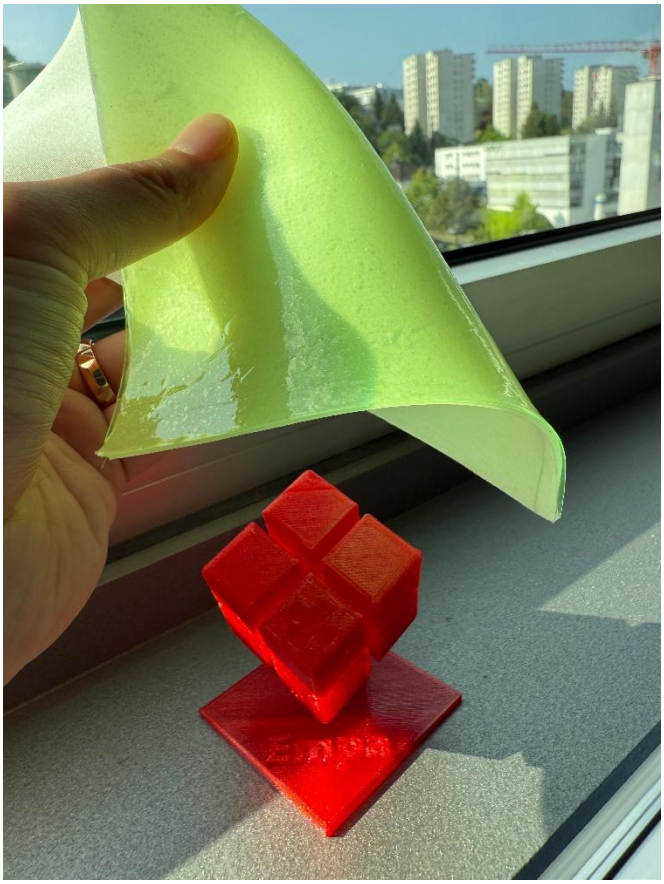

Publisher:
Swiss Federal Office of Energy SFOE
Energy Research and Cleantech
CH-3003 Berne
www.energy-research.ch

Subsidy recipients:
Empa
Lerchenfeldstrasse 5, St. Gallen, CH-9014
www.empa.ch

Schoeller Textil AG
Bahnhofstrasse 17, CH-9475 Sevelen
www.schoeller-textiles.com

Authors:
Luciano Boesel, Empa, luciano.boesel@empa.ch

SFOE project coordinators:
Michael Moser, michael.moser@bfe.admin.ch
Roland Brüniger, roland.brueniger@brueniger.swiss

SFOE contract number: SI/502457-01

Summary

In TeSK, we aimed at improving the properties of our flexible, wearable luminescent solar concentrators (wLSCs) and integrating them into textiles towards the development of truly textile energy harvesting systems. We evaluated the optical, mechanical, and stability properties of several systems and selected a formulation composed of a waterborne polymer and a water-soluble dye, both of which are already in use by the textile industry. The wLSCs could be prepared and incorporated on textiles using standard textile processing techniques (drop-casting and bar-coating). The final demonstrator was built using polyester as a base textile and polyurethane or siloxane as the guiding layer. Small-sized perovskite solar cell modules were chosen to be coupled to the wLSCs, both due to the matching of the wavelengths and to the flexibility of these modules. The textile energy harvesting system developed here could generate up to 5.7 W/m^2 of power density, corresponding to approximately 10% optical device efficiency, a value in line with the best rigid luminescent solar concentrators for building-integrated photovoltaics.

Zusammenfassung

Bei TeSK haben wir uns zum Ziel gemacht, die Eigenschaften unserer flexiblen und tragbaren lumineszierenden Solarkonzentratoren (wLSCs) zu verbessern und sie in Textilien zu integrieren, um textile Energiegewinnungssysteme zu entwickeln. Wir haben die optischen, mechanischen und stabilitätsbezogenen Eigenschaften mehrerer Systeme untersucht und eine Formulierung ausgewählt, die aus einem wasserbasierten Polymer und einem wasserlöslichen Farbstoff besteht, die beide bereits in der Textilindustrie verwendet werden. Die wLSCs konnten mit Hilfe von Standardverfahren der Textilverarbeitung (Tropfenabguss und Stabbeschichtung) hergestellt werden und in Textilien integriert werden. Der endgültige Demonstrator wurde unter Verwendung von Polyester als Basistextil und Polyurethan oder Siloxan als Führungsschicht realsiert. Aufgrund der spektralen Übereinstimmung und der Flexibilität dieser Module konnten die kleinen Perowskit-Solarzellenmodule mit den wLSCs gekoppelt werden. Das hier entwickelte textile Energiegewinnungssystem konnte eine Leistungsdichte von bis zu 5,7 W/m^2 erzeugen, was einer optischen Geräteeffizienz von etwa 10 % entspricht, ein Wert, der mit den besten starren lumineszierenden Solarkonzentratoren für gebäudeintegrierte Photovoltaik vergleichbar ist.

Résumé

Au sein du TeSK, nous avons cherché à améliorer les propriétés de nos concentrateurs solaires luminescents flexibles et portables (wLSC) et à les intégrer dans des textiles afin de développer de véritables systèmes de récupération d'énergie textiles. Nous avons évalué les propriétés optiques, mécaniques et de stabilité de plusieurs systèmes et avons sélectionné une formulation composée d'un polymère à base d'eau et d'un colorant hydrosoluble, tous deux déjà utilisés dans l'industrie textile. Les wLSC ont pu être préparés et incorporés dans des textiles à l'aide de techniques de traitement textile standard (drop-casting et bar-coating). Le démonstrateur final a été construit en utilisant du polyester comme textile de base et du polyuréthane ou du siloxane comme couche de guidage. De petits modules de cellules solaires en pérovskite ont été choisis pour être couplés aux wLSC, à la fois en raison de l'adéquation des longueurs d'onde et de la flexibilité de ces modules. Le système de collecte d'énergie textile développé ici pourrait générer jusqu'à 5,7 W/m^2 de densité de puissance, ce qui correspond à environ 10 % d'efficacité optique, une valeur conforme aux meilleurs concentrateurs solaires luminescents rigides pour les systèmes photovoltaïques des bâtiments.

Contents

List of abbreviations

SFOE = Swiss Federal Office of Energy

CAGR = compound annual growth rate

FSC = flexible solar cells

LSC = luminescent solar concentrator

NIR = near-infrared

PCE = power conversion efficiency

PDMS = polydimethylsiloxane

PNC = perovskite nanocrystal

SC = solar cell

LR = Lumogen red

BY40 = Basic Yellow 40

DR277 = Disperse Red 277

Tg = Glass transition

APCN = Amphiphilic polymer co-networks

HEA= Hydroxyethylacrylate

PDMS = methacryloxypropyl terminated polydimethylsiloxanes

PTFE = Polytetrafluoroethylene

PA = Polyamide

PES = Polyester

PU=Polyurethane

Si SCs=monocrystalline silicon SCs

DSSC=dye sensitized solar cells

CIGS PVC= copper indium gallium selenide Photovoltaic cell

OPV cells = Organic Photovoltaic cells

PSC= perovskite solar cells

ECE= external quantum efficiency

1 Introduction

1.1 Context and motivation

Portable electronic devices for communication, transportation, and sensing are being developed and used more and more frequently. Accordingly, the need for renewable and ubiquitous power sources that would allow these devices to be used anywhere, continuously, and without dependence on fixed power grids is growing. Photovoltaic technology is ideally suited for these purposes, due to its high efficiency and very good power handling capacity. The global market size for "portable solar cell-powered chargers" is expected to reach U$1.7 billion by 2025 (CAGR=21.3%). [Grand View Research, 2019. https://www.grandviewresearch.com/press-release/global-portable-solar-charger-market] Although flexible solar cells (FSC) can be combined with jackets, bags, tents, and other wearable textiles [1], their efficiency is much lower (maximum 25%) than solar cells (SC) for building technology (up to 47%). Moreover, their applicability is limited by lower spectral response, low efficiency under diffused light, and high cost per area. Nowadays, three types of FSCs are being investigated as wearable devices: perovskite SCs, dye-sensitized SCs, and organic SCs [1], [2]. However, to achieve high power conversion efficiency (PCE), these SCs must be produced by increasingly complicated synthetic methods. Moreover, it is required that such SCs maintain their PCE by about 80% after bending with a bending radius of up to 1mm, which is very demanding on the mechanical stability of the whole product. Therefore, there is a clear need to develop additional materials that make it easier to achieve these demanding goals. Luminescent solar concentrators (LSCs) can be the solution to this multifaceted challenge: they are flexible/bendable, easier to manufacture than FSCs, and can also be integrated into/on textiles (as fibers, in textile structures, or when finished as coatings). LSCs absorb sunlight and convert it to the wavelength that is optimal for the SC. This results in a geometric as well as a spectral concentration of the light. In addition, LSCs operate under diffuse or artificial light or partial shading [3], [4]. This results in increased efficiency and cost reduction for photovoltaic systems. Other advantages of LSCs are their color diversity, adaptability, and property adjustability [5]. Although rigid LSCs have been studied for building-integrated SC for 30 years, and many start-ups offer LSCs with glass as the substrate, research on textile-based, flexible, and wearable LSCs is virtually nonexistent.

The goal of this project is to build a demonstrator of a "power-generating textile". The textile will include 3 components: the substrate (textile itself), the LSC (either fiber-based or film-based), and FSC (coupled to the LSC). We will first describe this system in terms of their power output (in watts = W): both the FSC alone and the FSC-LSC together. Finally, we will connect the FSC-LSC demonstrator to a rechargeable device (e.g. smartphone or flashlight) and charge it with sunlight.

1.2 Project objectives

The aim is to answer the following questions at the end of the project: How much higher is the power output (W) from the FSCs when the LSCs are tied to it? What is the power output when the FSCs are not exposed to the sun at all, but are placed "hidden" behind the textiles, and receive the photons only through the LSCs? What is the efficiency of the LSC-FSC system compared to the FSC alone when the days are cloudy, or the light is diffuse?

2 Approach, method, results and discussion

2.1 Approach and Method

WP1 Material Selection

Siloxane-, urethane-, and acrylate-based resins

Synthesis of materials: the investigated polymers (siloxane-, urethane-, and acrylate-based resins) were prepared as per the manufacturer's recommendation. That means usually mixing a two-part resin and curing it under high temperature (up to 60°C) or UV light for 3 min. Moreover, a new type of urethane resin with a longer pot time (time until hardening) was ordered.

UV-Vis spectroscopy: blocks of the pristine resins were prepared with 1 cm size and their light transparency was evaluated from the UV to the near-infrared region (that is, 200 nm to 900 nm).

Fluorescence spectroscopy: films of the resins with different amounts of perovskite nanocrystals (PNCs) were prepared and their fluorescence was analyzed. For that, we choose the excitation wavelength of 365 nm and emission range of 480 nm to 560 nm. PNCs were added to the resins prior to their curing, to ensure good dispersion.

Waterborne LSCs

The acrylic acid ester and styrene polymer waterborne dispersion Revacryl P 7602 [6] (Synthomer PLC) was mixed with the water-soluble fluorophores Basic Yellow 40 (BY40) and Disperse Red 277 (DR277). The dispersion was chosen as the efficiency of those LSCs are comparable to established LSCs made of PMMA as host material and loaded with the dye Lumogen red F350 (LR) (BASF). Films were gained by letting the water evaporate in the open air. Furthermore, the di-functional water-soluble aliphatic urethane acrylate oligomer SWA 8084 (Solmer Soltech LTD) was used as an alternative as host matrix, due to its application in UV cured coatings. Further alternative polymer dispersions were the aqueous-self-crosslinking emulsions Plextol DV 245 and 455, which are based on acrylic polymer. The waterborne dispersions were mixed with the fluorophores BY40 and DR277.

Furthermore, for WP3 additional polymer dispersions as Textal PGS (Textilcolor AG), Tubicoat Wdd (CHT Germany GmbH), and Plextol DV 455 (Synthomer) were investigated. (see WP3 for details)

UV-Vis spectroscopy: samples with a thickness of around 1mm were prepared and their light transparency was evaluated from the UV to the near-infrared region (that is, 200 nm to 800 nm).

Double layer LSCs were prepared by fabricating two layers of either Revacryl P 7602 or SWA 8084 on top of each other on a glass slide. The bottom layer was 1mm thick and the top layer 200 µm. Only the top layer contained dye.

Fluorescence spectroscopy: films of the resins with different amounts of luminophores were prepared and their fluorescence intensity was analysed. Fluorophores dissolved in water were added to the resins prior to their curing, to ensure good dispersion.

Table 1 Excitation and emission wavelength of different luminophores.

Luminophore	Excitation wavelength [nm]	Emission wavelength [nm]
BY40	433	450-600
DR277	550	560-700

WP2 Fabrication of fiber-based LSCs

a) Molding of fibers

As mold a fluoroplastic tube (PTFE) was used, which was filled with either urethane- or acrylate-based resins. Polyurethane fibers were gained by curing them over night at room temperature. The Acrylate resin was polymerized via UV-light. After the curing step, the fibers were removed from the tubular PTFE molds leaving behind the optical fiber.

Fluorescence spectroscopy: films of the resins with different amounts of perovskite nanocrystals (PNCs) were prepared and their fluorescence was analyzed. For that, we choose the excitation wavelength of 365 nm and emission range of 480 nm to 560 nm. PNCs were added to the resins prior to their curing, to ensure good dispersion.

b) Microfluidic wet-spinning

We used a simple, cost-effective and fast microfluidic chip fabrication method previously developed in our group [7]. It is based on single-use stainless-steel hypodermic needles and the silicone elastomer PDMS. Besides the transparency of the spinneret, it stands out due to its flexibility in design adjustment. APCNs are covalently crosslinked hydrophilic and hydrophobic polymers, which form separated domains in the nanoscale and enable a continuous interface between the two polymers. For the hydrophilic phase HEA (Hydroxyethylacrylate, synthesized by our lab) was used and for the hydrophobic phase PDMS 50 (Polydimethylsiloxane, methacrylpropyl terminated, viscosity 50-90cst purchased from abcr). For all formulations 0.6wt% of the initiator Irgacure 651 was added. The APCN fibers were spun according to our patent WO2023/209037A1. The pre-polymers served as inner flow and a sodium alginate solution of 3 wt% as sheath flow. To ionic-crosslink the alginate a 7wt% $CaCl_2$ solution was used. The sodium alginate shell functions as mold for the pre-APCN fibers. A UV light source was implemented at the end, to induce crosslinking through photopolymerization. The core was extracted by introducing a NaCl solution to the system. The workup procedure developed in the group [7] for APCNs was applied to obtain solid polymer APCN fibers. The hydrophobic phase PDMS 50 was exchanged with DDDMA (1,12-Dodecanediol dimethacrylate). The flow rate of the core and the shell was 400 µL/min for APCN fibers. For the acrylate fibers the core flow rate was 100µL/min and the shell 100µL/min.

Attenuation measurements were performed with the optometer at a wavelength of 660nm for acrylate fibers. From 80 cm for every 10 cm until a length of 20cm remained, the attenuation was defined. Three different fibers were taken and each measurement was repeated three times at each length. The gained values were plotted in a graph and the slope of each obtained function was taken to determine the mean attenuation value.

WP3 Fabrication of film based LSCs & WP4 Integration of the LSCs and SCs in textiles

<u>LSC coatings with APCNs</u>

The synthesis of Amphiphilic polymer co-networks (APCNs) films was performed after a protocol, which was developed in our group. [8, 9, 10, 11] APCNs are covalently crosslinked hydrophilic and hydrophobic polymers, which form separated domains in the nano-scale and enable a continuous interface between the two polymers. Preliminary tests have shown, by applying a methacryloxypropyl terminated polydimethylsiloxanes (PDMS, abcr swiss AG) with high molecular weights. Therefore, PDMS125 with 10000 g/mol and PDMS1000 with 25000 g/mol were applied, with a ratio of 70:30 hydrophilic: hydrophobic phase results in films with increased adhesion on hydrophilic substrates. APCNs are waterproof and breathable membranes, which make them ideal for weather protective clothing as they are puncture resistant due to their elasticity and swelling ability in water, enabling self-sealing of the matrix. [8] A Polyamide (PA) and Polyester (PES) textile sample, provided by Schoeller were used as substrate. The

textiles were treated with plasma or the hdydrophilic agent Arristan Air (CHT Germany GmbH) to increase the hydrophilicity of the textiles and therefore enable an improved adhesion of the APCN films on the textile substrate. For the plasma treatment, the textiles were exposed to a gas mixture of 20 sscm argon and 5 sscm oxygen for 1min at 20 Watt and 7 Pascal. As an alternative method, the foulard is used to impregnate the textiles with a hydrophilic agent. With a wet pick-up of 72% at 6 bar per 4 m/min for Polyesters and 50% wet pick-up at 1 bar per 1m/min for PAs.

Untreated Polyamide textiles, provided by Schoeller, were directly coated with APCN membranes. The membranes contained 70wt% HEA and 30wt% PDMS1000. (Polydimethylsiloxane, methacrylpropyl terminated, viscosity 1000cst purchased from abcr) and 0.6wt% Irgacure 651 was added.

Double layer LSCs

For double layer LSCs, the aliphatic Polyurethane dispersion (PU) Textal PGS (Textilcolor AG) was applied on Polyester (PES) and Polyamide (PA). On top, Plextol DV 245 or Plextol DV 455 with 0.2wt% BY40 was applied to fabricate a 0.2µm LSC layer. Schoeller fabricated a variation of PU membrane thicknesses (Table 2), on which a 200µm layer of Plextol 455 was applied.

Table 2 PES and PA textiles coated with different thicknesses of PU (Textal PGS).

Fabric No	
Fabric 1	100% PA with 25µm Textal PGS layer
Fabric 2	100% PES with 1mm Textal PGS layer
Fabric 3	100% PES with 25µm Textal PGS layer
Fabric 4	Textal PGS (2mm thick) on PES
Fabric 5	Textal PGS (1mm thick) on PES

Before applying the LSC membrane, PES coated with PU was treated with the hydrophilic agent Arristan EPD (kindly provided by CHT Germany GmbH) to increase the hydrophilicity of the textiles and therefore enable an improved adhesion of the APCN films on the fabric. Two different techniques are used to impregnate the textiles with a hydrophilic agent: foulard and casting. For the foulard method, a wet pick-up of 25% was achieved at 1bar per 1m/min. For the casting method, 20mL Arristan EPD was poured on top of a PU film, coated on a PES textile. The respective fabric was fixed with metal blocks on top, to prevent the PU layer to run out (Figure 2). Excess water was evaporated in the open air and fixated at 170°C for 40s in a lab dryer for textiles. The desired film thickness was achieved by calculation and subtraction of evaporated water. The same procedure was repeated when using Arristan Air instead of Arristan EPD as hydrophilic agent.

Additionally, tests with alternative bottom layers were performed. Tubicoat Wdd (CHT Germany GmbH) as an alternative PU to Textal PGS (Textilcolor AG). PU Tubicoat WDD was not suitable as it flowed through the PES fabric. Therefore, Tubicoat WDD and Textal PGS were mixed with ratios of 1:3, 1:1, and 3:1. However, in all cases the Tubicoat WDD still flowed through the textile. Based on the experience of fabricating air bubble free films with Sylgard 184 in prior experiments, the Sylgard 184 siloxane was put under vacuum to remove the air bubbles (Figure 1a). The same observation of running through the fabric was made with the PDMS Sylgard 184 as well. As an alternative siloxane, which is used in textile industry for coating fabrics already, Tubcosil HAB5-1 was chosen, which kindly provided by CHT. To remove additional air bubbles the Tubcosil mixture stayed in membrane vacuum for 1.5h. Simultaneously air was removed from time to time before it was put in an ultrasonic bath for 10 minutes. Furthermore, PU Tubicoat Wdd (CHT Germany GmbH), siloxanes Sylgard 184 (Dow) and Plextol DV 455 (Synthomer) were chosen as alternative bottom layers on PES. As the Plextol samples leaked as well, we tried to seal the fabric by coating the wrong side of the fabric with a thin layer of Textal PGS. On the

right side of the fabric the Plextol DV 455 layer was then applied, showing no leakage. All coated films were treated with the hydrophilic agent Arristan Air to enable coating of the bottom layer with a LSC made of Plextol DV 455 containing 0.2wt% BY40. The bottom layers Textal PGS and Tubcosil HAB 5-1 were coated with the LSC mixture. For Textal the direct coating of the LSC layer was successful (Fabric 6). However, the film exhibited a heterogeneous wetting behavior with non-uniform coating of the hydrophilic LSC layer compared to Fabric 2 and Fabric 3, when the Textal layer was thinner. In thicker films the water evaporation might lead to the development of microcracks and therefore reduce the uniformity in surface coating. We selected Tubcosil due to its good light-guiding character and hydrophobicity, in order to test an alternative method of attaching LSCs. As wetting of the surface with the LSC layer was not possible, due to its hydrophobicity, the LSC layer was fabricated separately on a glass plate (Figure 3) and then contact-pressed on top of the Tubcosil bottom-layer. To ensure strong adhesion, the Textal PGS-, Tubcosil HAB 5-1, and Plextol DV 455-surfaces were activated with Plasma to adhere them to a LSC made of Plextol 455 containing 0.2wt% BY40. For the plasma treatment the chamber Aurora 350 (serial No 11365) from Plasmatreat was used with the parameters 139sccm argon and 99sscm oxygen, using a radio frequency plasma generator that outputs 300watts of power. However, adhesion was only achieved with Plextol (fabric 13 and fabric 15) as bottom layer.

Table 3 Different PU-, siloxane-, and acrylic polymer bottom layers on PES either without or with Plextol 455 containing 0.2wt% BY40 as LSC. All samples had the size of 11.5x17.5cm.

Fabric No	
Fabric 6	Textal PGS (1mm thick) on PES with directly applied LSC (0.1mm thick)
Fabric 7	Textal PGS on PES (1mm thick) with LSC (0.22mm thick) put on top manually
Fabric 8	Tubcosil HAB 5-1 (3.6mm thick) on PES
Fabric 9	Tubcosil HAB 5-1 (3.6mm thick) on PES with LSC (0.3mm thick) put on top manually
Fabric 10	Tubcosil HAB 5-1 (0.9mm thick) on PES
Fabric 11	Tubcosil HAB 5-1 (0.9mm thick) on PES with LSC (0.07mm thick) put on top manually
Fabric 12	Plextol DV 455 (1.5mm thick) on PES
Fabric 13	Plextol DV 455 (1.5mm thick) on PES with LSC (0.14mm thick) adhered through plasma treatment
Fabric 14	Plextol DV 455 (2mm thick) on PES
Fabric 15	Plextol DV 455 (2mm thick) on PES with LSC (0.11mm thick) adhered through plasma treatment

a) 

Figure 1 a) Sylgard 184 and Tubcosil HAB5-1 were put in a desiccator to remove the air bubbles before coated on PES.

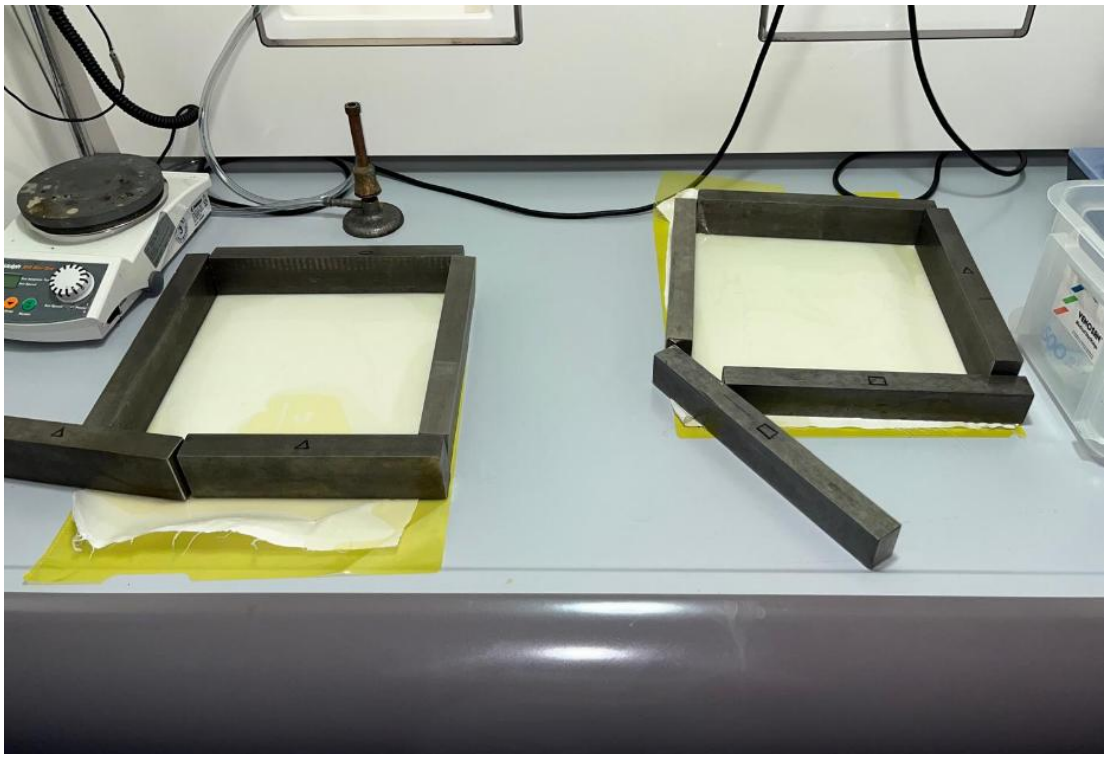

Figure 2 Textal PGS applied on PES trough drop casting.

Figure 3 LSC Plextol 455 with 0.2wt% BY40 on a glass plate.

Samples of 1x1cm of 200µm thick LSCs based on Plextol DV455 and 0.2wt% BY40 coated on fabric two were put in water (Table 4). The leakage of the dye BY40 and detachment of the LSC layer is investigated.

Table 4 Leakage experiments with 1x1cm big samples of LSCs made of Plextol DV455 and 0.2wt% BY40 applied on fabric 2.

Sample No	Amount of water [mL]	Temperature [°C]
Sample 1	30	25
Sample 2	10	40

The fluorescence intensity of the water was measured at the excitation and emission wavelength of BY40 at different days.

Afterwards the samples were dried to investigate the attachment of the LSC on the fabric.

Leakage tests were performed with LSCs on glass slides based on Revacryl P 7602 and SWA 8084 containing DR277 as dye to test the stability of the respective polymer in water and its delamination behaviour.

WP5 "Proof-of-concept" Studies

With the Empa self-build solar cell demonstrator first proof of concept measurements were performed (Figure 4) with ceiling light (10-40 W/m^2) and a torch (Chameleon CU 6 from Nitecore) of an area of 415.5 mm^2 with 2.04kW/m^2. Therefore, a PVCs based on crystalline silicon with as measurement of 20.3cm x 16cm were built into the solar demonstrator (Figure 4). The measured power, voltage or current can be read from the display or a laptop screen with the Empa self-programmed software, which is connected via USB cable.

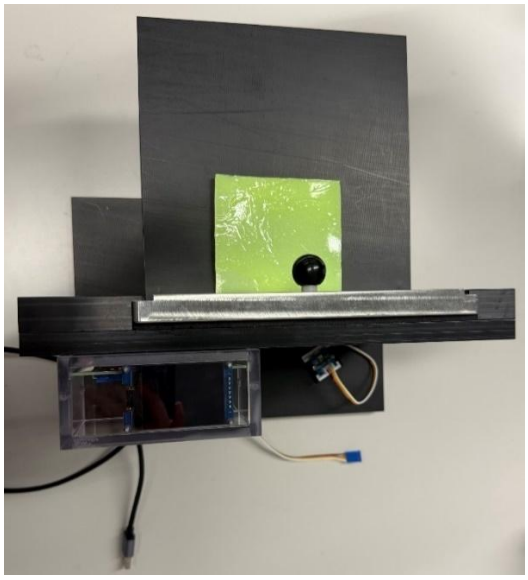

Figure 4 Solar cell demonstrator with a LSC made of Plextol 455 and 0.2wt% BY40 on fabric 2.

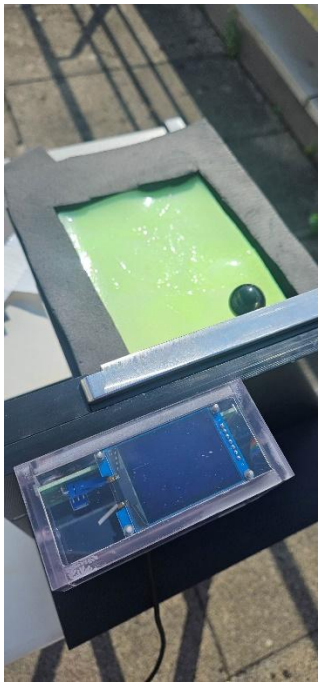

Figure 5 Solar cell demonstrator for outdoor measurements. Around the sample a black foam frame was put to ensure, that no additional light reaches the solar cells.

The Inkjet-Printed PSCs (perovskite solar cells) built into the demonstrator (Figure 5), were purchased from Saule Technologies. It contains two PCSs, hidden behind a metal plate (Figure 6), with the respective size of 56.2mmx15mm each. The samples had dimensions of 11x18cm. For the indoor measurement, the radiation power of the 205W lightbulb at a distance of 41cm from the sample was determined via the optometer P9710 (Gigahertz Optik), using a photodetector wavelength range of 400-1000nm. For the outdoor measurement the measured global radiation averaged over ten minutes was taken from the homepage of the Federal Office of Meteorology and Climatology MeteoSwiss.

https://www.meteoschweiz.admin.ch/service-und-publikationen/applikationen/ext/daten-ohne-programmierkenntnisse-herunterladen.html#lang=de&mdt=normal&pgid=&sid=&col=&di=&tr=&hdr=

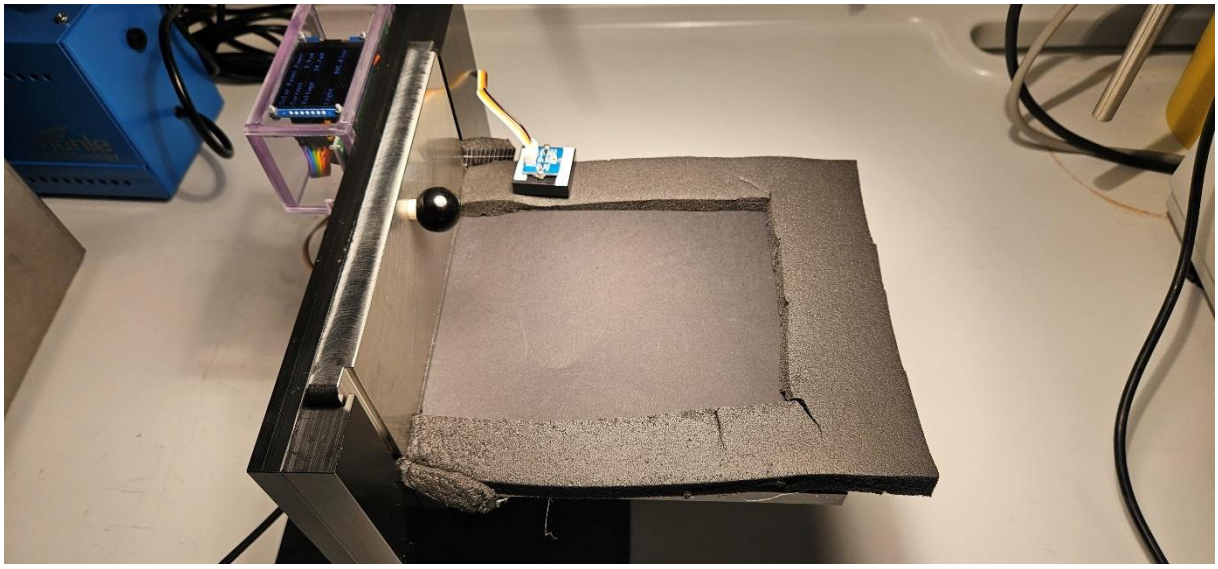

Figure 6 Black paper was put on top as reference measurement to ensure, that the generated power is solely generated by the samples.

As reference, the samples were covered with black paper (Figure 6), to ensure that any generated power was derived solely through the LSC layer and not because any light can pass through a slit to hit the solar cell directly.

For the calculation of the power output density, the measured output power was taken times the area. The area was determined by multiplying the combined length of the two solar cells times the thickness of the double layer LSC without the thickness of the fabric. For the thickness a mean of 0.195mm was calculated.

2.2 Results and Discussion

WP1 Material Selection

The UV-Vis spectra of two types of resins show that both are highly transparent in the visible and NIR regions (above 400nm) and present equivalent properties (Figure 7). Siloxane presents better transmittance in the UV region, and has additionally a longer pot-life, making it easier to prepare the LSCs for future tasks.

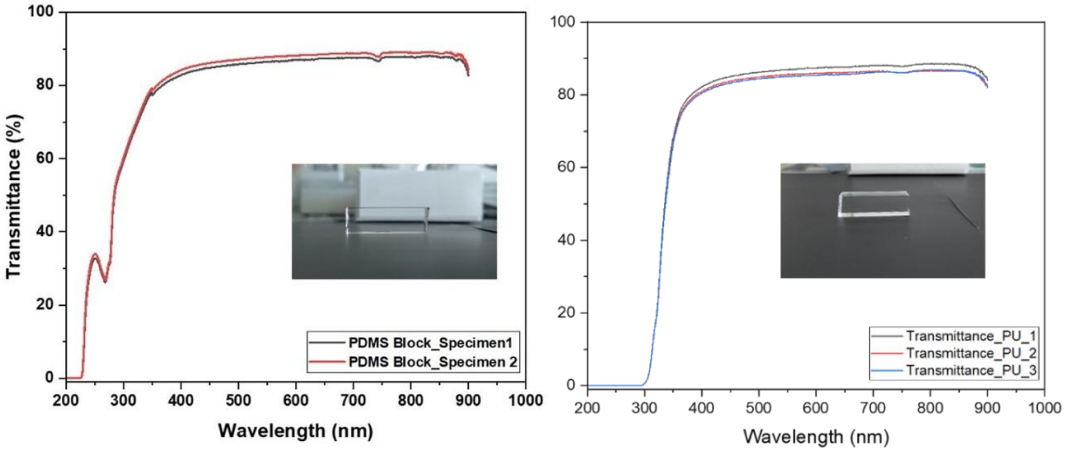

Figure 7 Left) UV-Visible-NIR spectrum of a 1 cm block made of siloxane resin (polydimethylsiloxane, PDMS). The inset shows a photo of the block. Right) UV-Visible-NIR spectrum of a 1 cm block made of urethane resin. The inset shows a photo of the block.

The three types of resins were mixed with varying amounts of PNCs, and their fluorescence was measured (Figure 8). The results showed the typical self-quenching behavior of fluorophores, that is, an increase of fluorescence intensity until a maximum is achieved at a certain concentration. Above this value, the PNCs quench too strongly and the fluorescence decreases. The maximum fluorescence was achieved at the following concentrations: 0.15 % (urethane resin), 0.07 % (acrylate resin), and 0.03 % (siloxane resin).

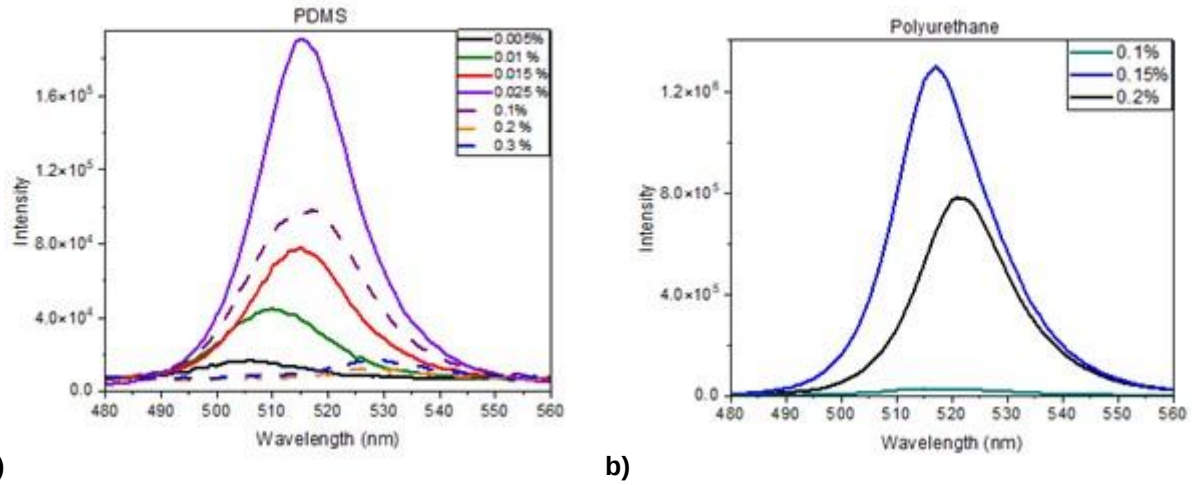

a) **b)**

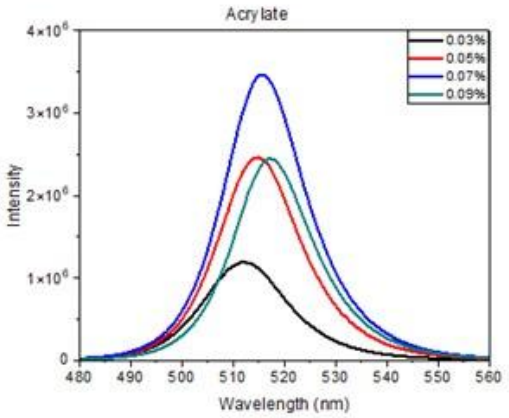

c)

Figure 8 a) Evolution of the fluorescence intensity of PNCs in siloxane resin as a function of PNC concentration. 5 replicates were measured for each composition, and only the median is shown. b) Evolution of the fluorescence intensity of PNCs in urethane resin as a function of PNC concentration. 5 replicates were measured for each composition, and only the median is shown.

The UV-Vis spectra of Revacryl P 7602 (Figure 9a) and SWA 8084 (Figure 9b) show the high transparency of both resins in the visible region and therefore their suitability for our application. SWA 8084 has a slightly higher transmittance with 20% than Revacryl P 7602 with 11.5% in the UV region.

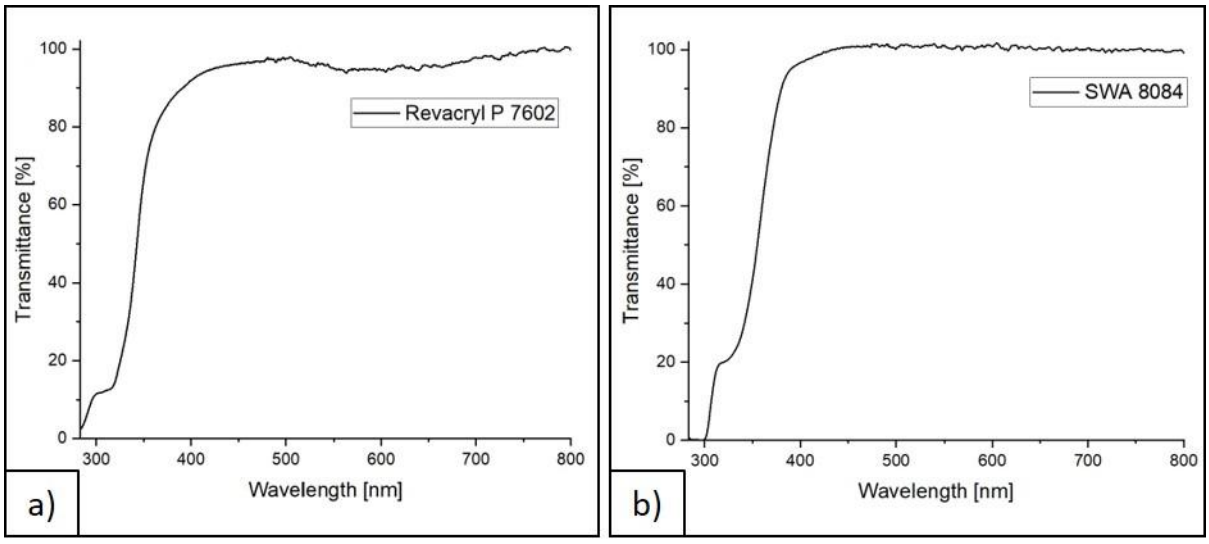

Figure 9 a) UV-Vis spectrum of a 1mm film made of Revacryl P 7602. b) UV-Vis spectrum of a 1mm film made of SWA 8084.

Two different dyes- Coumarin 6 and LR305- at varying amounts were mixed with PDMS and their fluorescence was determined (Figure 10). The fluorescence increases until a maximum is reached and declines afterwards due to the self-quenching behavior of fluorophores. The maximum fluorescence was achieved at 0.02 wt% Coumarin 6 and 0.02 wt% LR305.

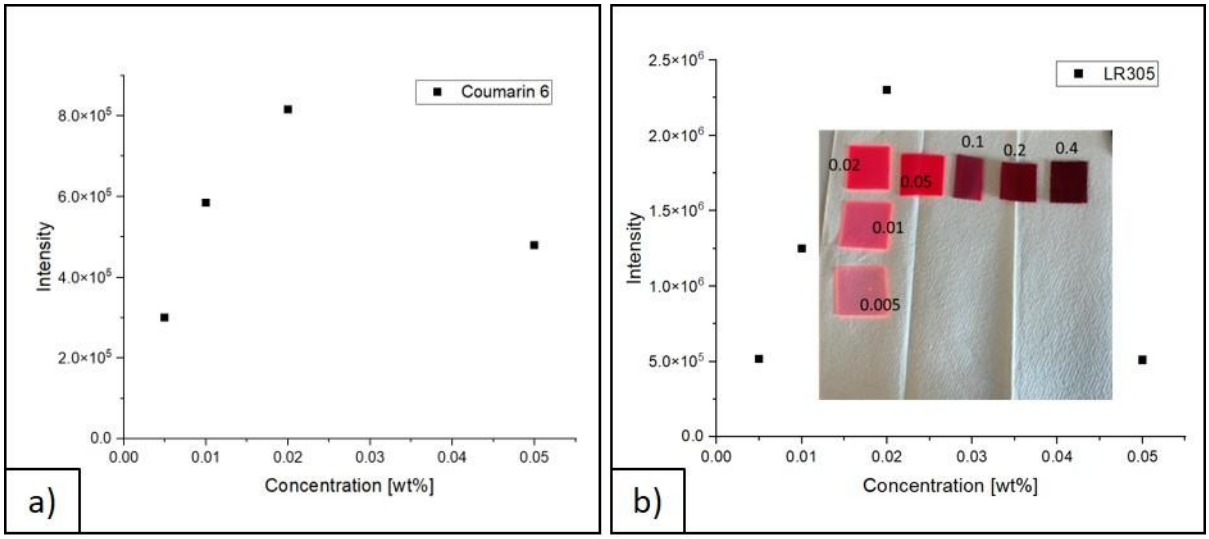

Figure 10 a) Maximum photoluminescence emission intensity of various Coumarin 6 concentrations in PDMS. Only the median is shown. b) Maximum fluorescence intensity of different LR305 concentrations in PDMS. Only the median is shown.

Revacryl P 7602 was mixed with different concentrations of BY40 (Figure 11a). The films were cured in the open air for 2h (black rectangle) and the median is shown as 3 replicates were measured. Additionally, the films were annealed (red dots) overnight in a vacuum oven at 60°C subsequent to the polymerization in the air. The annealing process does not influence fluorescence behavior. The maximum fluorescence was achieved at 0.1 wt% BY40. The same process was conducted for dye DR277 (Figure 11b). The maximum fluorescence was measured at 0.05 wt% DR277. SWA 8084, another waterborne polymer, was used as host matrix. Preliminary tests show that for BY40 the maximum value was reached at 0.1 wt% as well (Figure 11c), whereas for DR277 the highest fluorescence intensities were reached with concentrations of 0.05 wt% and 0.1wt%.

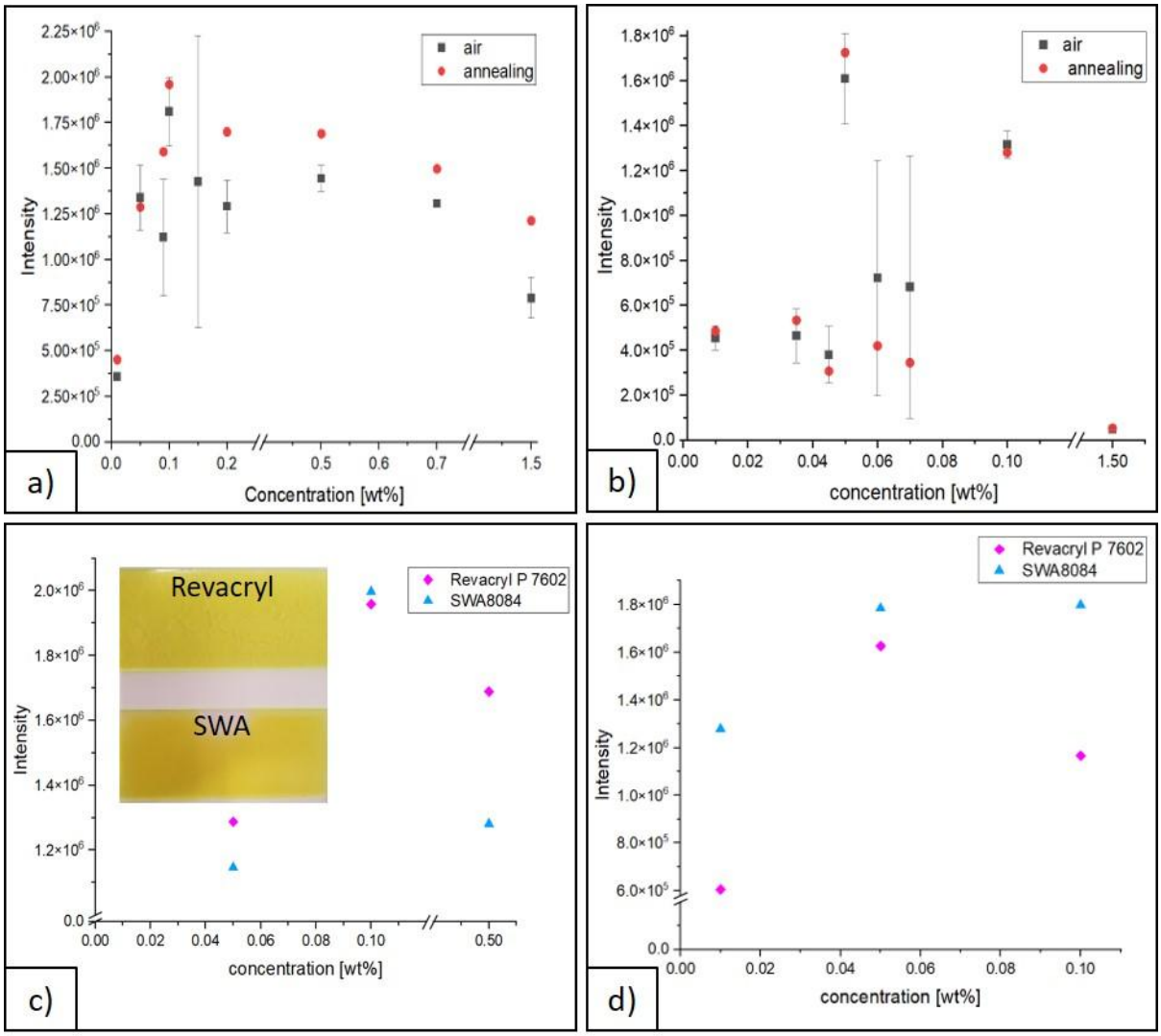

Figure 11 a) Maximum photoluminescence emission intensity of numerous BY40 concentrations in the waterborne polymer Revacryl P 7602 after polymerization in air or with additional annealing after polymerization. b) Maximum photoluminescence emission intensity of numerous DR277 concentrations in Revacryl P 7602 after polymerization in air or with additional annealing after polymerization. c) Maximum fluorescence intensity of various BY40 concentrations in two different waterborne polymers. d) Maximum fluorescence intensity of various DR277 concentrations in two different waterborne polymers.

Double layer LSCs made of Revacryl P 7602 and SWA 8084

For Revacryl P 7602 (Figure 12a) and SWA 8084 (Figure 12b), applying a double layer instead of using a single layer is advantageous as the fluorescence intensity stays more unform with increasing distance. However, by applying two layers of either Revacryl or SWA on top of each other, the surface starts to get indentations for Revacryl or wrinkles for SWA (Figure 12c). It was expected to have better light guidance through the bottom layer. These non-uniform surfaces probably influence the intensity of the guided light, leading to the overall low values for double layer LSCs. Furthermore, samples containing SWA and DR277 (Figure 12b, red) showed an irregular distribution of the red dye.

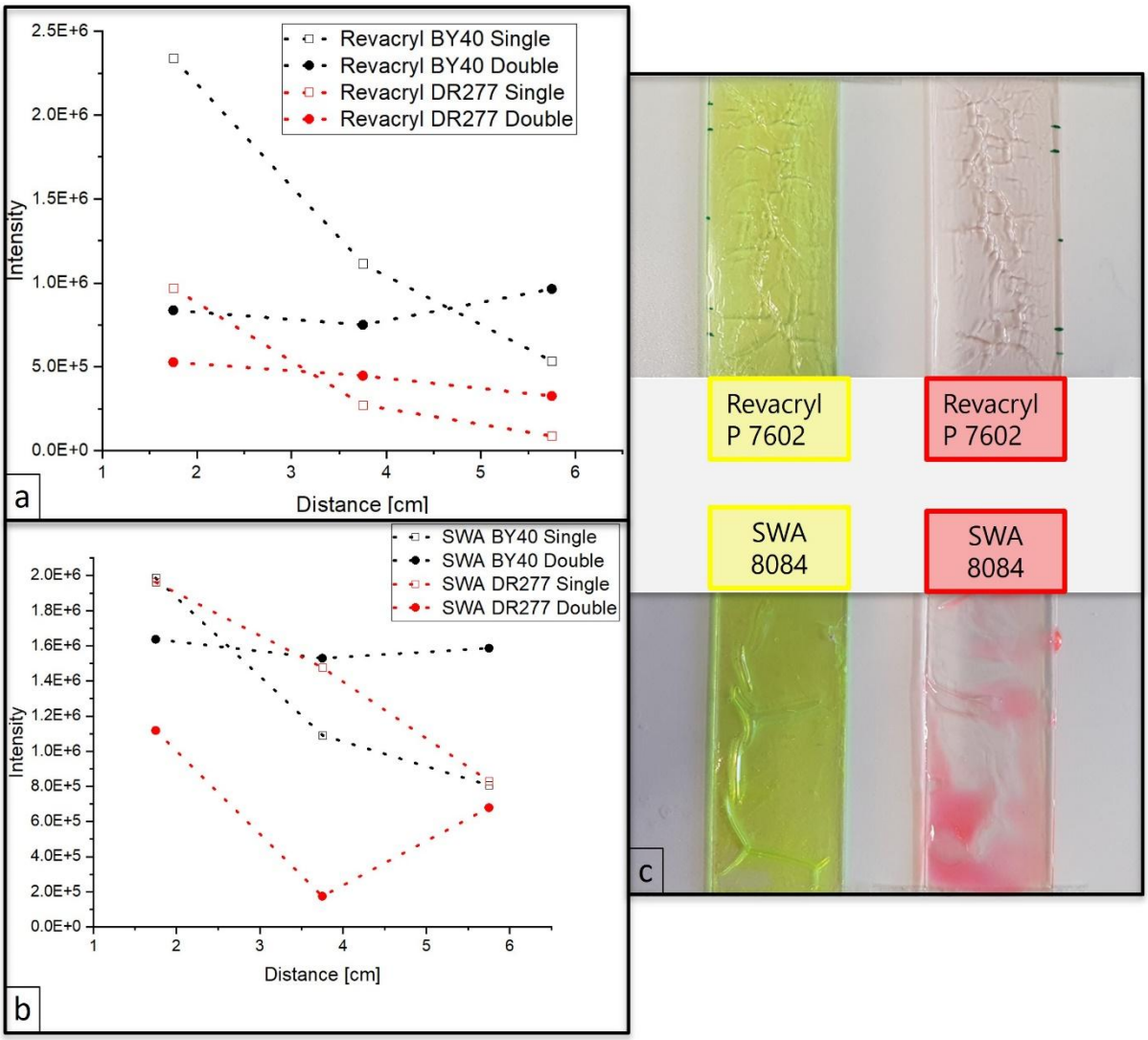

Figure 12 Double layer LSCs. a) Double layer LSCs prepared with two layers of Revacryl P7602. The films either contained BY40 (black curve) or DR277 (red curve). b) Double layer LSCs prepared with two layers of SWA 8084. The films either contained 0.1wt% BY40 or 0.05wt% DR277 as dye. c) Double layer LSCs made out of Revacryl P 7602 or SWA 8084 containing BY40 (yellow, left side) or DR277 (red, right side).

Leakage Test of waterborne LSCs based on Revacryl P 7602 and SWA 8084

Leakage tests were exemplary conducted with LSCs based on Revacryl P 7602 and SWA 8084 containing DR277 as dye. For the calibration curve (Figure 13a), different concentrations of DR277 were dissolved in water (Figure 13b) and their fluorescence intensity was measured.

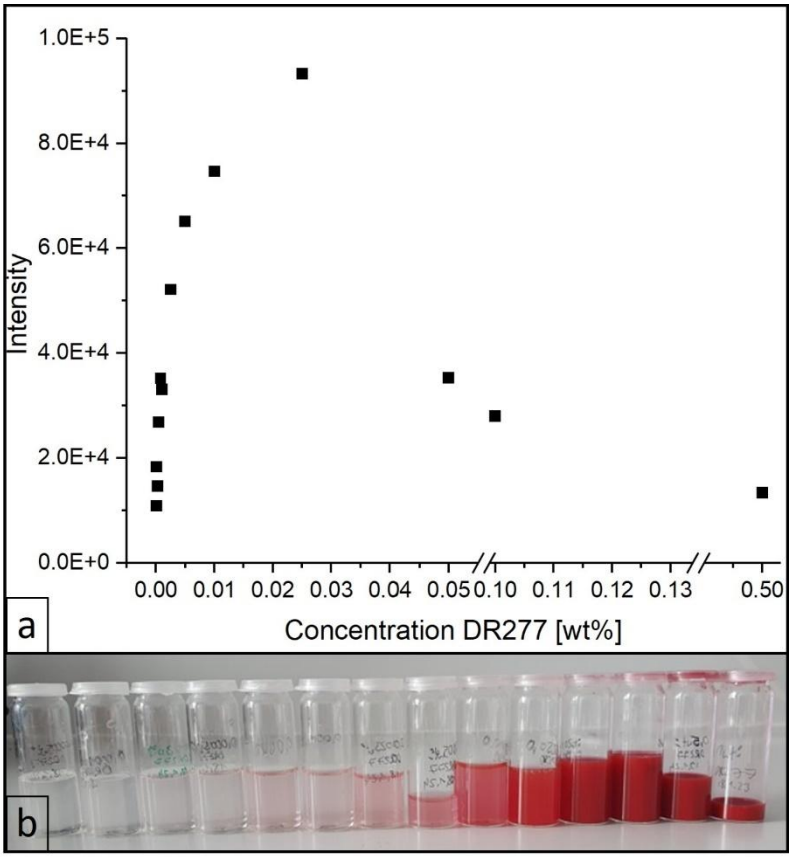

Figure 13 Calibration curve. a) Different concentrations of DR277 and its respective fluorescence intensity. b) Different concentrations of DR277 dissolved in water.

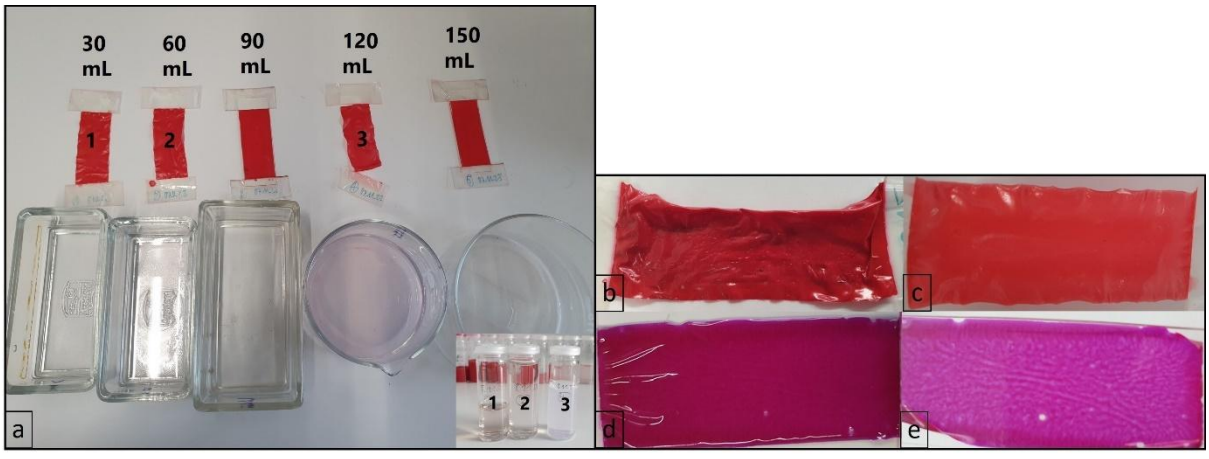

Figure 14 Leakage Test. a) Samples with Revacryl P 7602 containing 1.5wt% BY40 were put in water for one week. b) Revacryl sample after drying at 40°C in an oven. c) Revacryl film after drying in a vacuum oven. d) LSC containing SWA 8084 with 1.5wt% DR277 was put for one week in water. e) SWA film after drying at 40°C in an oven.

LSCs made of Revacryl and 1.5wt% DR277 were put into different amounts of water for one week (Figure 14a). Although the samples were covered with a lid, water evaporated for the water baths containing 90mL and 150mL water. Therefore, the fluorescence intensity of water was only determined for

the samples one to three (Figure 14a). After one week in water, the surface of the Revacryl LSCs became uneven (Figure 14a). After drying in an oven at 40°C the films didn't recover their initial evenness (Figure 14b). Therefore, the samples were dried in a vacuum oven to ensure the evaporation of water (Figure 14c). Even then, the films did not go to their initial surface appearance. For films containing SWA the surface did not lose its evenness (Figure 14d). The films were dried in an oven at 40°C (Figure 14e). All LSCs made of Revacryl P 7602 delaminated from the glass slides. The ratio for the amount of fluorophore solution to the combined amount of polymer and fluorophore solution was 1:2.5. The results show, for sample 2 a total of 0.7% DR277 was released. For sample 3 a maximum of 1.7% DR277 was released from the total dye amount in the specimen. For the other samples no value was determined, as they were higher than the values in the calibration curve (Figure 13).

Table 5 Leakage Test. Revacryl P7602 and SWA 8084 LSCs containing DR277 were put for one week in different amounts of water. The fluorescene intensity of the respective water baths were measured.

Sample No	**Dye (DR277) concentration [wt%]**	**Polymer**	**Water amount [mL]**	**Film weight [g]**	**Fluorescence intensity**	**Amount of DR277 released from the total amount of dye in the film [%]**
1	1.5	Revacryl P7602	30	0.139	1.38*10^5	
2	1.5	Revacryl P7602	60	0.144	7.19*10^4	~0.7
3	1.5	Revacryl P7602	120	0.156	1.05*10^5	~1.7
4	1.5	SWA 8084	30	0.141	2.10*10^5	
5	0.1	SWA 8084	30	0.157	4.56*10^5	

Single layer Plextol DV 245 and Plextol DV 455

Due to the stickiness of SWA 8084 films and that LSCs based on Revacryl P 7602 change their surface's evenness, it was necessary to find an alternative polymer. Synthomer provided us with aqueous emulsions of a self-crosslinking acrylic polymer Plextol DV 245 with a glass transition Tg of -33°C and Plextol DV 455 with a Tg of 16°C.

For the first trial Plextol DV 245 and 455 films were loaded with 0.1wt% BY40 and the fluorescence intensity was measured with 3 different distances between light source and detection of the fluorometer (Figure 15a). All experiments were conducted with BY40 as dye, as prior results with Revacryl P 7602 show a higher intensity. This is supported by literature [6].

Overall, Plextol DV 455 shows a higher fluorescence intensity compared to Plextol DV 245, which is attributed to the higher light transmission of Plextol DV 455 (Figure 15b).

To find the ideal concentration regarding highest fluorescence intensity, films made of Plextol DV 245 and 455 were loaded with different concentrations of the dye BY40 ranging from 0.05wt% to 1wt% (Figure 16). Samples containing 0.1-0.3wt% BY40 for both polymers had the highest fluorescence intensity. For further experiments 0.2wt% BY40 was chosen.

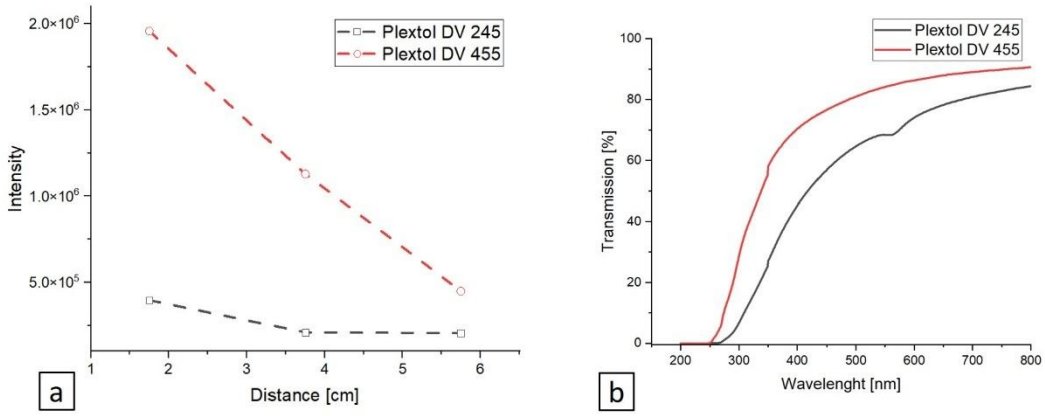

Figure 15 Figure 5 Single layer Plextol DV 245 and 455 films. a) Fluorescence intensity of Plextol DV 245 and 455 films containing BY40 at different distances. b) UV-Vis spectrum of Plextol DV 245 and 455.

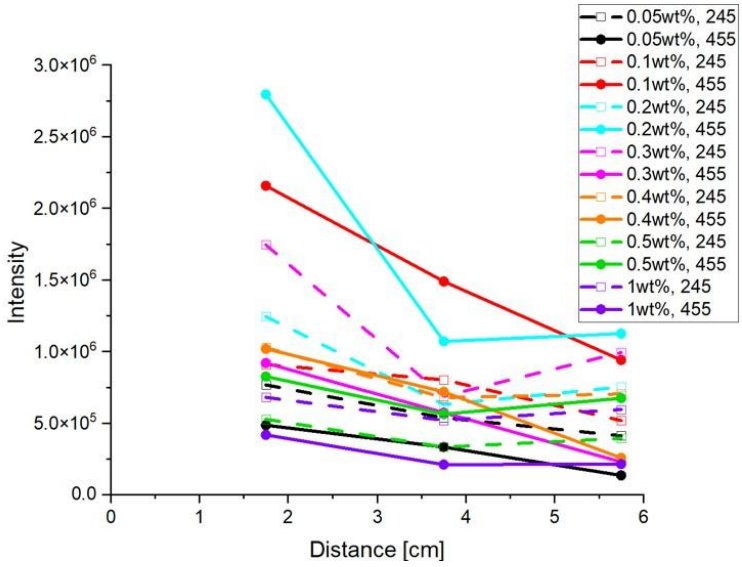

Figure 16 LSC films containing Plextol DV 245 or 455 and different concentrations of BY40. Measured at different distances.

WP2 Fabrication of fiber-based LSCs

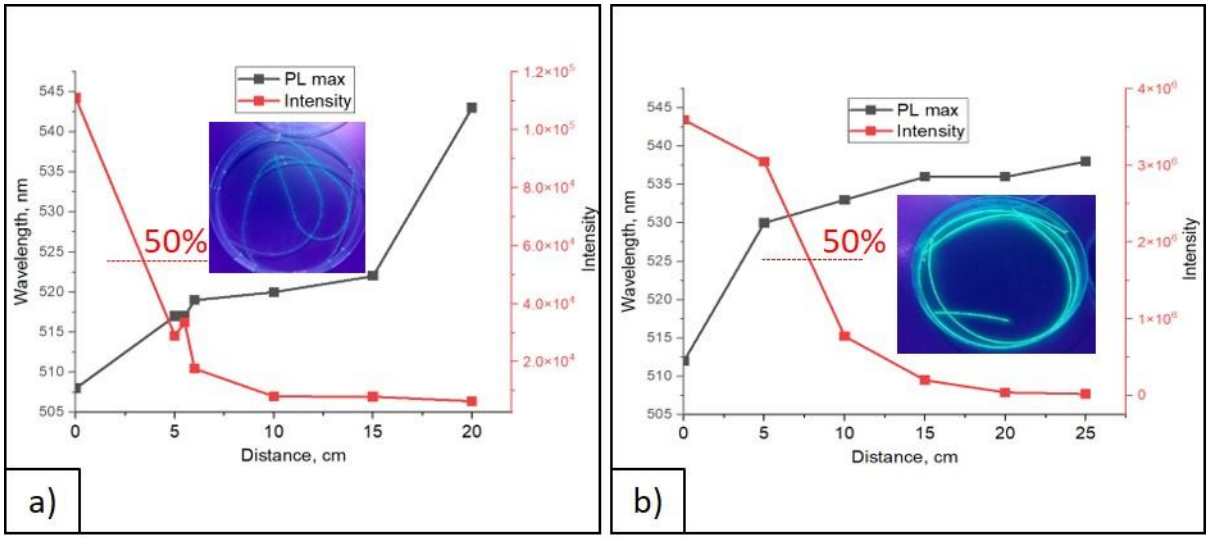

Figure 17 a) Perovskite nanocrystals embedded in a molded Polyurethane fiber. b) Perovskite nanocrystals loaded on acrylate fibers generated by molding.

With increasing distance from the detector, hence with increasing fiber length the fluorescence intensity decreases. This could be attributed to host absorption loss, photon escaping and self-absorption. [9] A red-shift occurs with increasing path length due to photon recycling. [10] The shift is more pronounced for Polyurethane fibers (Figure 17a) compared to acrylate fibers (Figure 17b), where a plateau is reached within a fiber length of 15 to 25 cm. For acrylate fibers 30m long fibers were spun.

For Acrylate fibers spun through microfluidic spinning an attenuation of 0.14 ± 0.016 dB/cm was determined, which met our goals with reaching an attenuation lower than 0.3 dB/cm (Figure 18b).

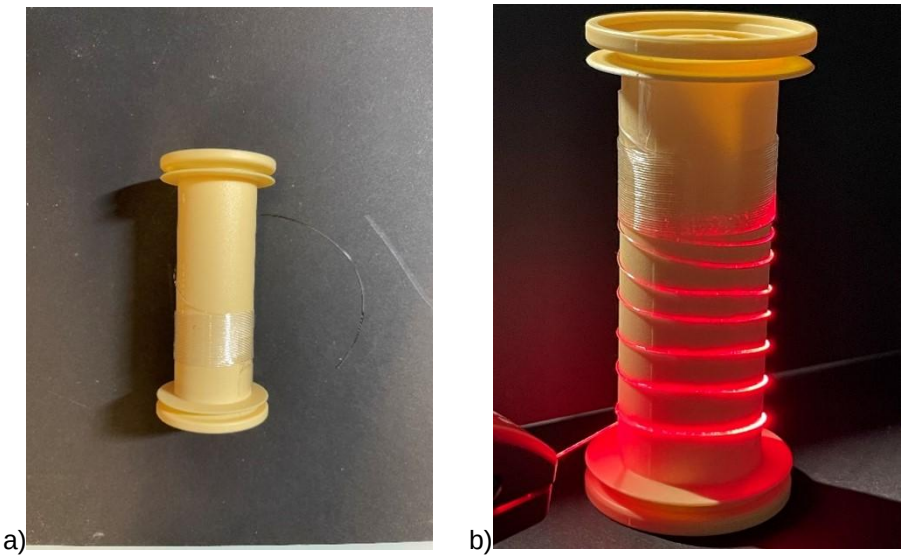

Figure 18 a) Microfluidic spun acrylate fibers rolled up on a spool. b) Light guided through an acrylate fiber obtained from microfluidic spinning.

APCN fibers were spun through microfluidic wet-spinning with a length of up to 48 cm. Optical measurements were performed to evaluate the light transmission of the fibers. The light is well transmitted. The ripples created many light loss points which lead to low light outputs. APCN fibers have the potential to be integrated into textiles.

Pre-APCN fibers were spun via microfluidic wet spinning. APCNs made of 30wt% HEA and 70wt% PDMS50 were spun with a core flow of 400µL/min and shell flow of 600µL/min. The end of the core capillary and the end of the shell capillary were 0.8cm apart. Exemplary a spun fiber of 40cm is shown (Figure 19).

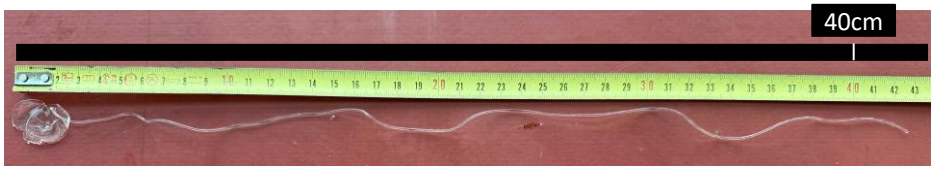

Figure 19 Exemplary spun APCN fiber made of 30wt% HEA and 70wt% PDMS50.

However, the spinning of APCN fibers with a composition of 30wt% HEA and 70wt% PDMS50 were not reproducible. Therefore, the formulation was changed to 50wt% HEA and 50wt% PDMS50 to ensure Newtonian fluid behavior, so that a stable flow is enabled by preventing viscosity changes of the polymer fluid during the spinning process. Fibers with a length between around 90cm to 210cm were spun reproducibly (Figure 20) when using a core flow of 400µL/min and shell flow of 600µL/min.

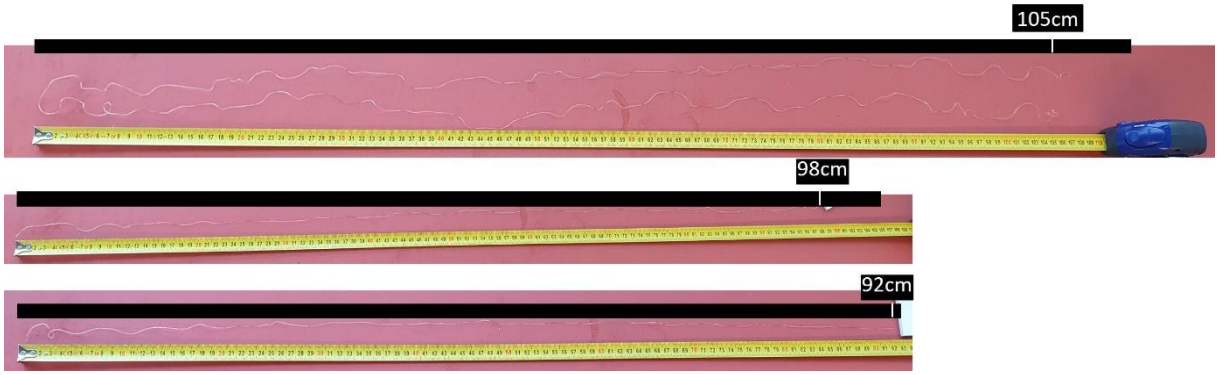

Figure 20 APCN fibers made of 50wt% HEA and 50wt% PDMS50.

The hydrophobic phase PDMS50 was exchanged with DDDMA, which has a 4 times lower viscosity than PDMS50. Due to the lower molecular weight of DDDMA, the fibers are stiffer compared to the fibers containing PDMS50. Fibers with lengths of about 20cm were spun (Figure 21).

Figure 21 APCN fiber made of 30wt% HEA and 70wt% DDDMA.

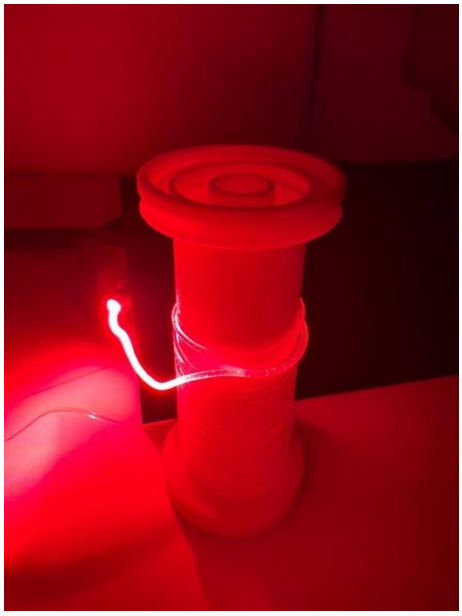

Figure 22 Light guided through an APCN fiber obtained from microfluidic spinning.

For APCN fibers an attenuation ranging from 0.24896 dB/cm (R^2=0.45489) to 0.38312 dB/cm (R^2=0.56056) was determined.

WP3 Fabrication of film based LSCs &

WP4 Integration of the LSCs and SCs in textiles

APCNs

APCNs based on two different PDMS with different molecular weights were attached to an untreated Polyamide or Polyester textile, provided by Schoeller. PDMS1000 with a molecular weight of 25000g/mol showed a very good adhesion on Polyamide (Figure 23a) compared to Polyester (Figure 23c). For PDMS125 with a molecular weight of 10000g/mol, the adhesion was poor for both fabric types (Figure 23b & Figure 23d). According to literature, higher adhesion energy is observed for PDMS with high molecular weights. This is attributed to the increased number of longer free chains, which benefit substrate wetting at a molecular scale. This leads to an elevated energy dissipation during detachment due to chain movements. Chain motions and rearrangements enable an improved chain absorption onto the substrate and therefore more interactions occur. [11] Furthermore, both APCN film types showed a poor adhesion on Polyester, which could be attributed to the higher hydrophobicity of Polyester fabrics compared to Polyamide.

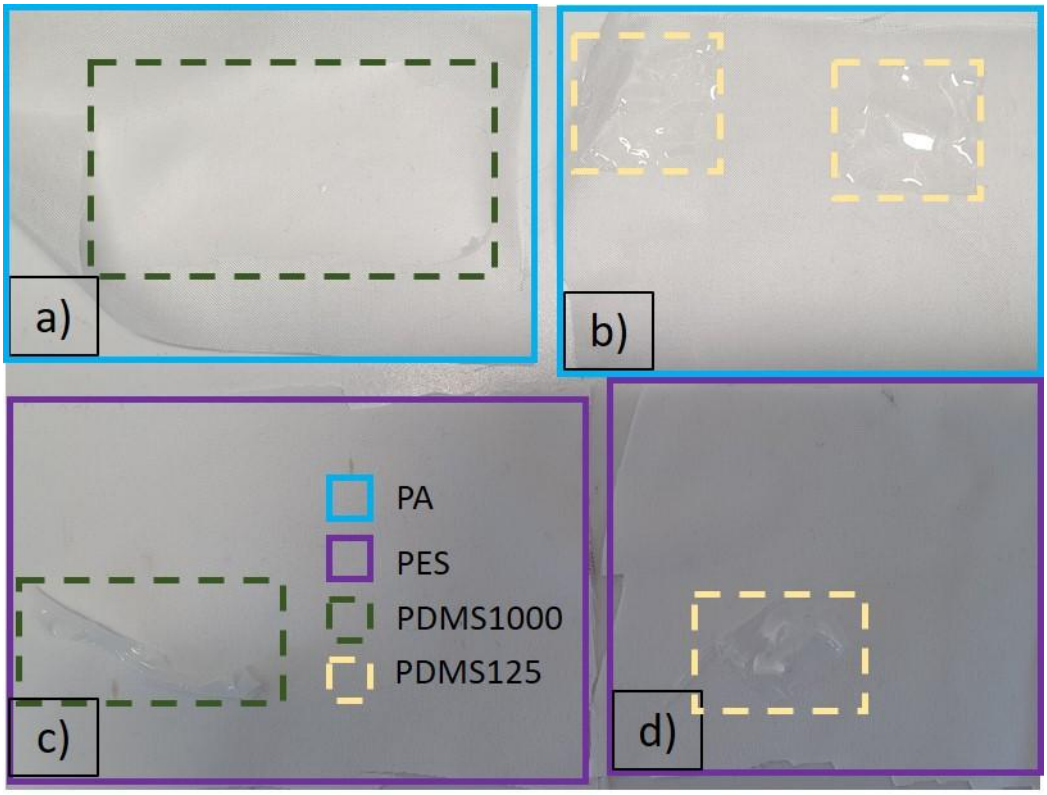

Figure 23 a) Polyamide textile coated with an APCN film based on PDMS1000. b) An APCN film, made out of PDMS125 is attached to a Polyamide fabric. c) Polyester textile coated with an APCN film based on PDMS1000. d) An APCN film, made of PDMS125 is attached to a Polyester fabric.

For the combinations, which showed bad adhesion of the APCN films (Figure 23b, Figure 23c and Figure 23d), the substrates were treated with plasma in advance, to increase the hydrophilicity of the fabrics. Except for the APCNs based on PDMS125 adhered on Polyester (Figure 24b), a very good adhesion was achieved for the other combinations (Figure 24a and Figure 24c).

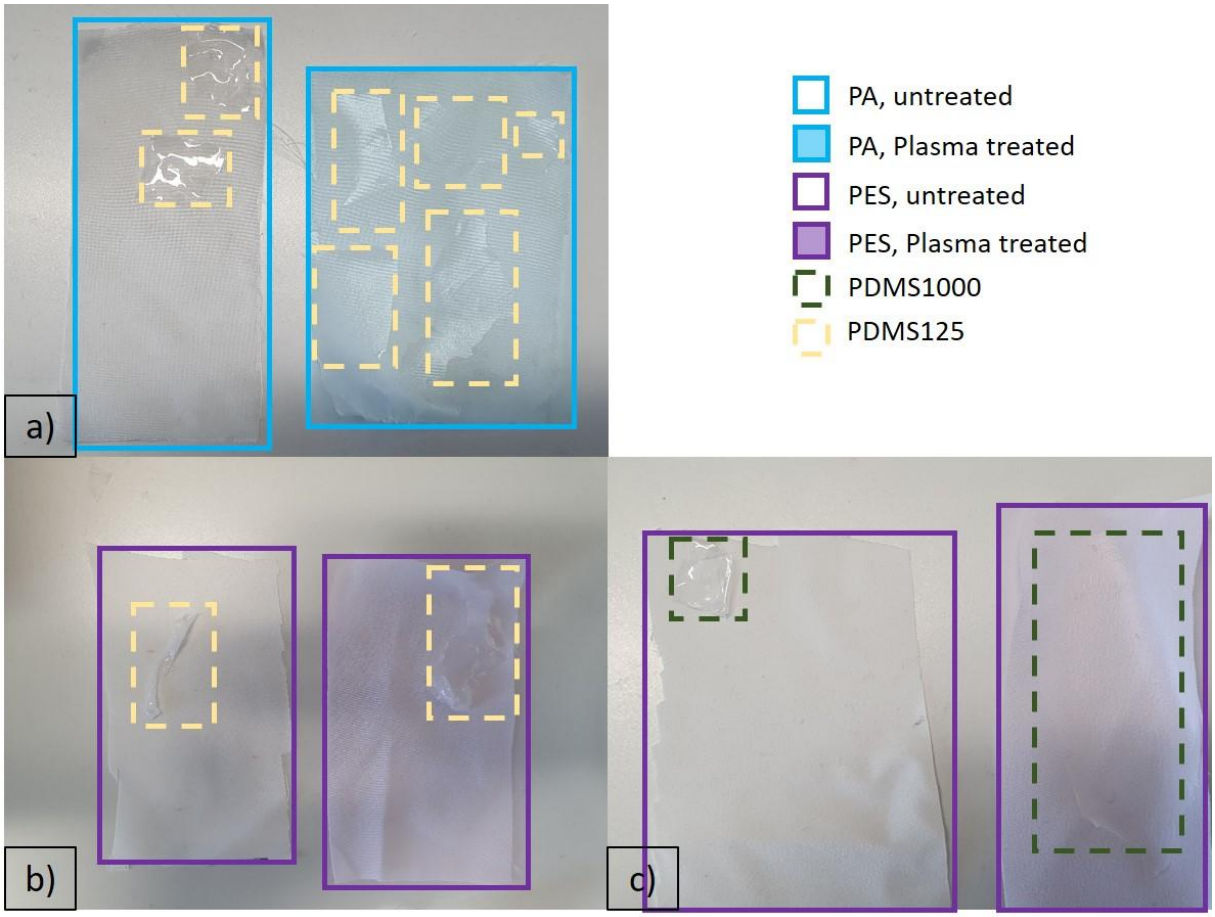

Figure 24 a) Attachment of an APCN based on PDMS125 on a plasma treated (right side) Polyamide fabric. b) Attachment of an APCN based on PDMS125 on a Polyester fabric, the textile was treated with plasma (right side). c) Comparison of the adhesion behavior of an APCN film based on PDMS1000 on a Polyester fabric without plasma treatment (left side) and treated with plasma (right side).

Adhesion was successful for all APCN films on both fabric types, which were pre-treated with the hydrophilic agent Arristan Air (Figure 25).

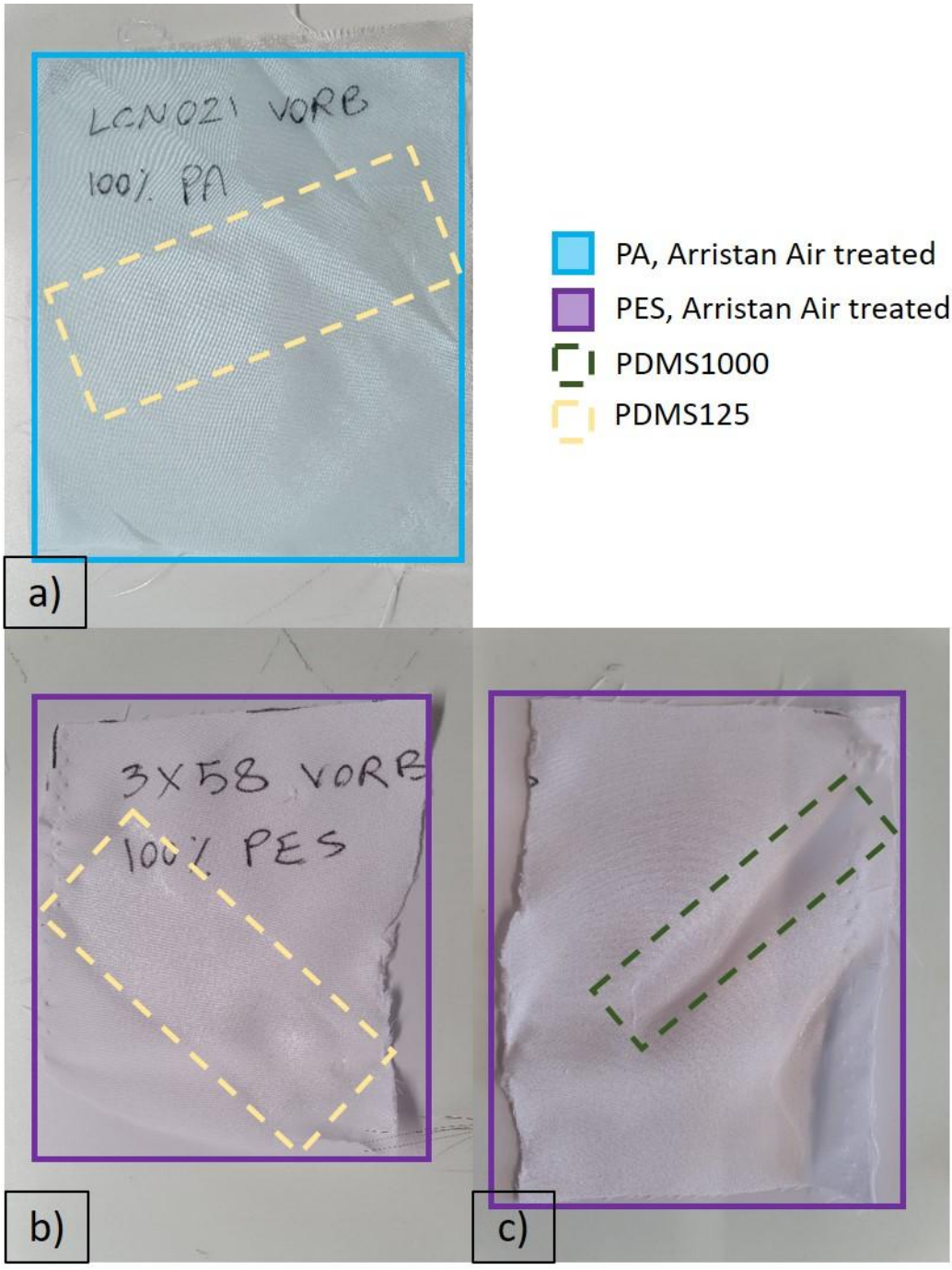

Figure 25 a) Attachment of an APCN based on PDMS125 on a Polyamide fabric pretreated with the hydrophilic agent Arristan Air. b) Attachment of an APCN based on PDMS125 on a Polyester fabric pretreated with the hydrophilic agent Arristan Air. c) Adhesion of an APCN film based on PDMS1000 on a Polyester fabric, prior treated with the hydrophilic agent Arristan Air.

Single layer APCN membrane on Polyamide

According to literature, higher adhesion energy is observed for PDMS with high molecular weights. This is attributed to the increased number of longer free chains, which benefit substrate wetting at a molecular scale. This leads to elevated energy dissipation during detachment due to chain movements. Chain motions and rearrangements enable an improved chain absorption onto the substrate and therefore more interactions occur [11]. APCN membranes based on PDMS1000 were attached to an untreated Polyamide textile, provided by Schoeller (Figure 26). A solution of 0.1wt% BY40 was applied.

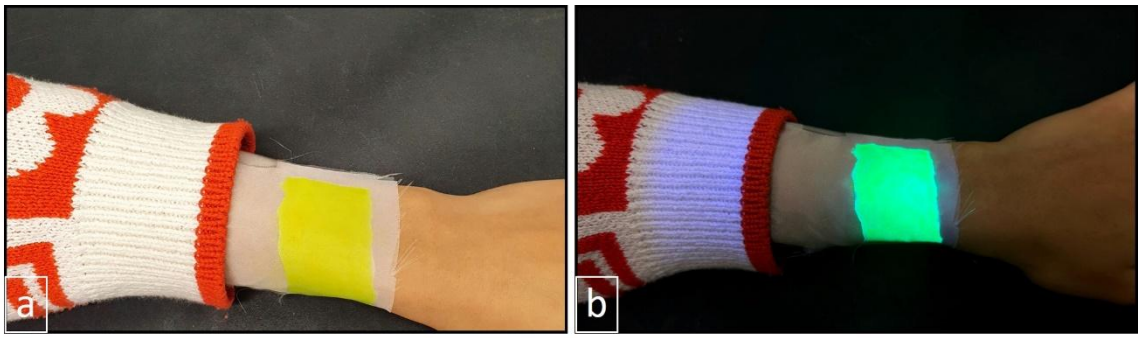

Figure 26 APCN membrane made of PDMS1000 was directly attached to an untreated Polyamide textile. a) At daylight. b) Illuminated in a dark room with a torch.

Double layer LSC with Polyurethane and Plextol DV

A 200µm layer of Plextol DV 455 (Figure 27a) or Plextol DV 245 (Figure 26b) with 0.2wt% BY40 was applied on top of fabric 1. Fabric 1 is made of PA and is covered with a 25µm PU layer. It was treated with the hydrophilic agent Arristan EPD before applying the LSC layer. It was not possible to fabricate uniformly even LSC films made of Plextol 455 (Figure 27a) and Plextol DV 245 (Figure 27b). Probably, the PU layer was not sufficiently hydrophilized leading to an agglomeration of the LSC layer. Due to Plextol DV 455 higher transparency, further experiments were continued solely with Plextol DV 455. Fabric 2 was not treated with the hydrophilic agent Arristan EPD (Figure 27c) and in Figure 27d treated with the hydrophilic agent in advance. By pre-treating fabric 2, the LSC layer could be evenly applied. The same result was found for fabric 3, where the pre-treatment with the hydrophilic agent (Figure 27f) led to an even LSC layer compared to not treating it in advance (Figure 27e).

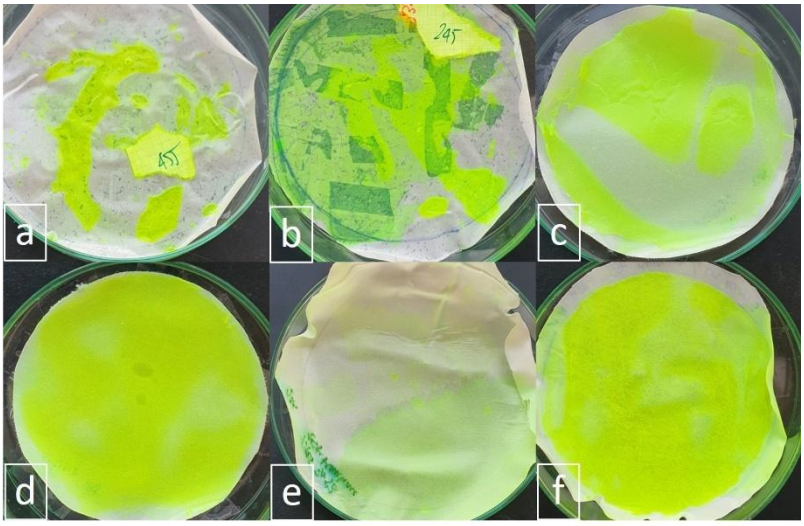

Figure 27 a) Plextol DV 455 on Fabric 1 with hydrophilic agent Arristan EPD. b) Plextol DV 245 on fabric 1 treated with hydrophilic agent Arristan EPD. c)Plextol DV 455 on fabric 2 treated with hydrophilization. d) Plextol DV 455 on fabric 2 without hydrophilization. e) Plextol DV 455 on fabric 3 without hydrophilization. f) Plextol DV 455 on fabric 3 with hydrophilization.

However, to guarantee efficient light guiding, an air bubble free PU layer of 1mm is required. Therefore, trials at Empa were performed using a bar coater or vacuum to fabricate PU films made of Schoeller's in-house recipe. However, it was impossible to get rid of the air bubbles. Therefore, trials in Schoeller's laboratory were performed. Manually with a doctor blade, PES fabrics were coated with PU. Printing oil was added to the Textal PGS mixture, which led to a decrease in air bubbles (Fabric 4). The best results were obtained when adding Textal Entschäumer K (Fabric 5) and by letting it stir continuously with the Textal PGS.

At Schoeller water vapor permeation (EN ISO 11092) was tested for the samples containing Textal PGS as bottom layer on PES, which was around zero. A fabric coated with PU was washed 5 times at 30°C (EN ISO 105-C06) and no detachment was observed. The above-mentioned experiments with the LSC layer attached to the Textal PGS were not possible to conduct due to the liquidation of Schoeller in Sevelen this summer.

Furthermore, PDMS Tubcosil HAB 5-1 (CHT Germany GmbH), and an aqueous emulsion of a self-crosslinking acrylic polymer Plextol 455 (Synthomer) were chosen as bottom layer alternatives to Textal PGS. They were coated on PES. Due to the restrictions mentioned in chapter 2.1 (WP3), the alternatives PU Tubicoat Wdd (CHT Germany GmbH) and PDMS Sylgard 184 (Dow) were not further investigated. As LSC layer Plextol DV 455 with 0.2wt% BY40 was chosen.

To test the detachment and washability of waterborne LSCs based on Plextol DV 455, sample 1 was put in water at room temperature and sample two was heated at 40°C in a benchtop shaking incubator (Table 4). The water, in which Sample 1 or Sample 2 were put in, did not show any color change after the leakage experiments were ended. After 24 hours sample 1 showed (Figure 28a) no fluorescence intensity. After seven days (Figure 28b) the signal changes and the formation of a noisy peak can be seen. However, due to the high noise of the peak even after 18 days (Figure 28c), the release of BY40 is very low. To determine the approximate amount of released BY40, the fluorescence intensity of different amounts of BY40 in water were measured (Figure 29). For sample 1, the amount of released BY40 is between 0.01% (Figure 29a) and 0.035% (Figure 29b) of the total amount of BY40 in the specimen. Samples from Figure 29c to Figure 29f can be excluded, as those samples were strongly yellowish colored from the dye BY40. Sample 2 did not show any change after 15 days (Figure 28f).

After drying the samples in the open air, no delamination or change of the surface was visible.

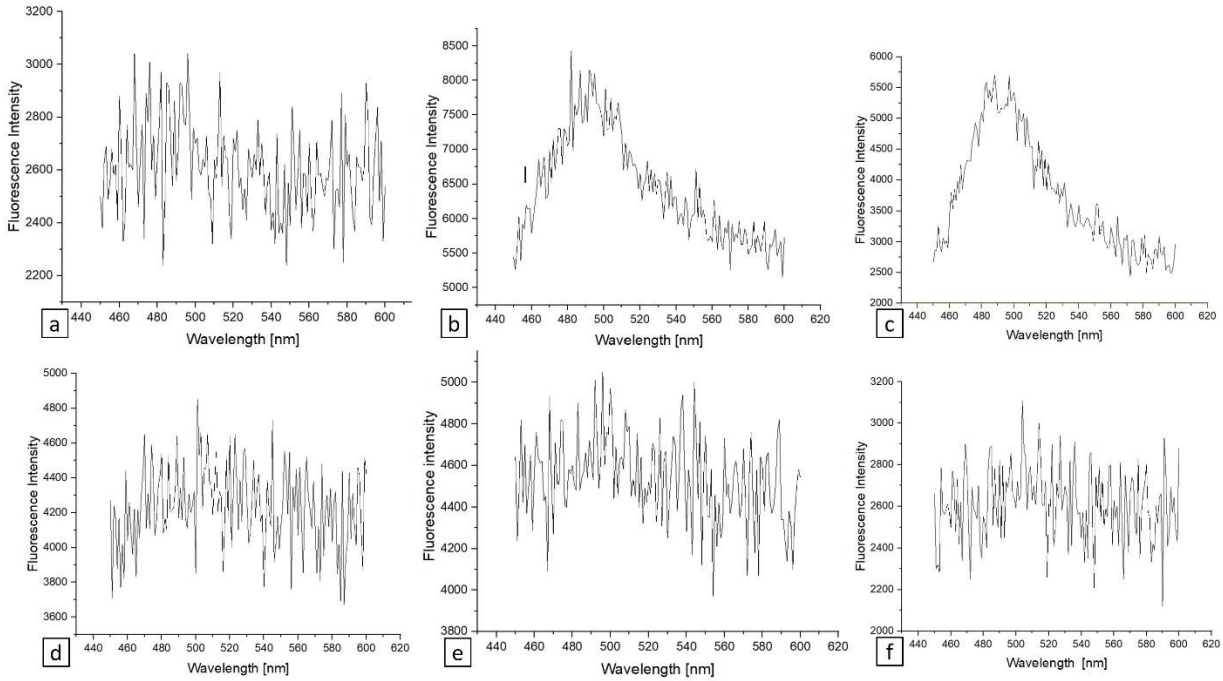

Figure 28 Leakage Test of LSCs based on Plextol DV 455 with 0.2wt% BY40 on fabric 2. a) Sample 1 after 24 hours in water. b) Sample 1 after 7 days in water. c) Sample 1 after 18 days in H2O. d) Sample 2 after 24 hours in water. e) Sample 2 after 7 days in water. f) Sample 2 after 15 days in water.

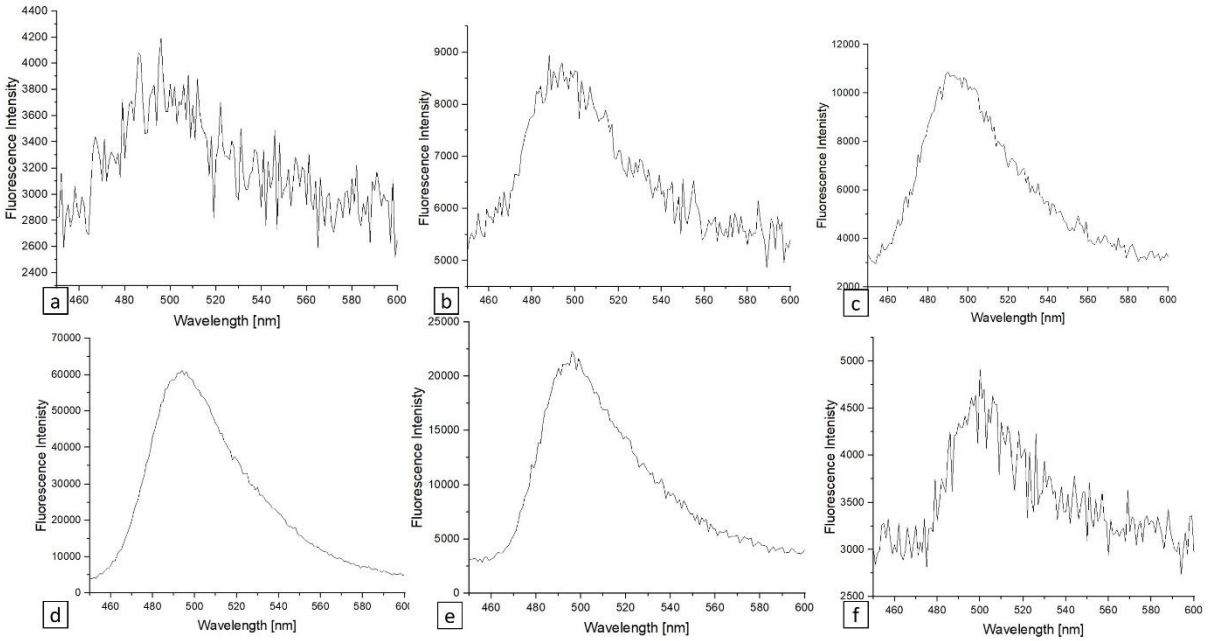

Figure 29 Measurement of the fluorescence intensity of different concentrations of BY40 dissolved in water. a) 0.00002wt% BY40. b) 0.00007wt% BY40 in water. c) 0.0002wt% BY40 in water. d) 0.002wt% BY40 in water. e) 0.01wt% BY40 in water. f) 0.02wt% BY40 in water

WP5 "Proof-of-concept" Studies

A power of 0.009 µW is generated, when a blank glass slide is illuminated (Table 6, sample 1). Sample 2 to sample 5 are LSCs, which were prior made in our laboratory, and were measured for comparison purposes. The double layer LSCs made of Revacryl P 7602 (Table 6, sample 7 & sample 11) and SWA 8084 (Table 6, sample 9 & sample 13) showed minor or no improvement regarding generated power compared to the respective single layer samples. This could be attributed to the uneven surface of the samples (Figure 12c) therefore preventing the undisturbed guidance of the light. Sample 14 (Table 6) shows promising energy harvesting results. Nearly twice as much energy was generated with sample 14 compared to sample 15, as Plextol DV 455 shows a higher transparency than Plextol DV 245 (Figure 15b).

Table 6 Measurements with the solar demonstrator containing PVCs based on crystalline silicon with as measurement of 20.3cm x 16cm. With an input of 5V DC and 0.1A. And a maximum output of 5V DC and 1A. Samples were illuminated with an irradiance of 2.04 kW/m^2 and with an area of 415.5mm^2.

Sample	**Sample No**	**Sub-strate**	**Dye**	**LxW [cm]**	**Current [µA]**	**Voltage [µV]**	**Power [µW]**
Glass slide	1	-	-	7.5x2.5	1	10.2	0.009
PDMS	2	-	0.02wt% LR 305	10x10	9.1	100.3	0.937
PDMS	3	-	0.02wt% LR 305	6x10	2.3	24.4	0.053
PDMS	4	-	0.02wt% Coumarin 6	10x10	3	31.9	0.088
Acrylate NOA83H	5	-	0.02wt% LR 305	5.3x4.4	19.4	102.6	0.938
Revacryl P 7602 single layer	6	Glass slide	0.1wt% BY40	6x2.5	1.9	20.8	0.039
Revacryl P 7602 double layer	7	Glass slide	0.1wt% BY40	6x2.5	3	33.1	0.1
SWA 8084 single layer	8	Glass slide	0.1wt% BY40	6x2.5	2.3	24.2	0.048
SWA 8084 double layer	9	Glass slide	0.1wt% BY40	6x2.5	1.8	19.2	0.032
Revacryl P 7602 single layer	10	Glass slide	0.05wt% DR277	6x2.5	0.3	3.4	0.001
Revacryl P 7602 double layer	11	Glass slide	0.05wt% DR277	6x2.5	0.5	5.5	0.003
SWA 8084 single layer	12	Glass slide	0.05wt% DR277	6x2.5	0.5	5.2	0.002

SWA 8084 double layer	13	Glass slide	0.05wt% DR277	6x2.5	0.3	2.9	0.001
Plextol DV 455	14	Glass slide	0.1wt% BY40	6x2.5	3.1	33.4	0.099
Plextol DV 245	15	Glass slide	0.1wt% BY40	6x2.5	2	22.1	0.043

To build a LSC demonstrator, commercially available solar cells are necessary, to incorporate them into the textile. Therefore, various companies were contacted. Besides standard silicon PV and CIGS (copper indium gallium selenide) PV, we also considered the emergent PV which hold potential for wearable applications: perovskite solar cells (PSC), dye sensitized solar cells (DSSC), and organic photovoltaics (OPV).

As a starting point, the thin solar cells IXOLAR from Anysolar were used. However, these monocrystalline silicon SCs (Si) are not ideal. Although they are thin and efficient (PCE=25%), they are not flexible and therefore not ideal for applications in textiles. Furthermore, our dyes (Table 1) are not ideally covered by the absorption range of Si-SCs (Figure 30a, b). CIGS are thin film solar cells (Figure 30a). The company SolarCloth only offered panels, which are slightly bigger than an A4 sized sheet. For initial proof of concept studies, they are too big and smaller cells are needed. With OPV (Organic Photovoltaic) cells from the Dresden based company Heliatek, we had the same issue. The cells were too big. Furthermore, they were not suitable for textile applications as they are not flexible. The Swedish company Exeger, which holds a licence of the DSSCs from the Grätzel lab (DSSC) [12], offers another type of thin film solar cells (Figure 30b). Unfortunately, they do not deliver any cells to non-strategic partners. Perovskia Solar, a Swiss spin-off from Empa, offers PSCs, but they are not compatible with textile applications. Saule Technologies (a Polish start-up originated from the Grätzel lab) offers Inkjet-Printed PSCs. PSCs (Figure 30c) show a stable absorption range between 450 and 600 nm. Therefore, the following proof of concept studies were performed with PSCs from Saule Technologies.

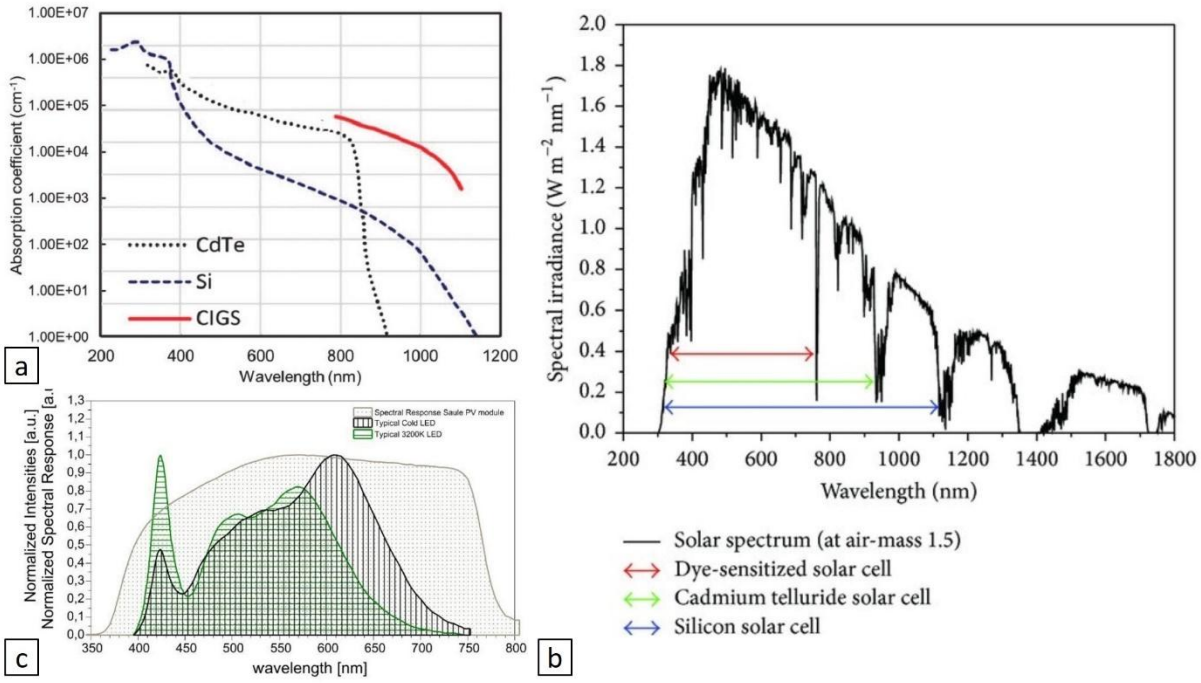

Figure 30 a) Absorption spectrum of CdTe, Si and CIGS solar cells [13]. b) Absorption spectrum of DSSC, Cadmium telluride and Si SCs [14]. c) Spectral response of Perovskite PV modules from Saule Technologies.

The PSCs showed promising results after preliminary measurements. The aim was to build a film-based LSC demonstrator by sewing the solar cells from Saule Technologies on the back of a jacket with the aid of the St Gallen-based tailor "Simis-Atelier für Mode+Design". Unfortunately, 1.5 months after placing an order, the order was suddenly cancelled. Even after several trials to get in touch with Saule Technologies within that period to ask about the whereabouts of the order. Later, we learned that the company is facing major legal issues with one of its investors and is entering bankruptcy; therefore, no solar cells could be delivered anymore. Consequently, no film-based LSC demonstrator was built. Due to the approaching deadline of this project, there was no time to test the suitability of alternative solar cells. Thus, the measurements were performed with the in-house-built solar cell demonstrator (Figure 5) containing two of the PSCs from Saule Technologies.

Tables 7 to 18 below present the results of measurements under different irradiation conditions: direct sunlight, diffuse sunlight, or indoor light. For each measurement, the average sun irradiance (obtained from https://www.meteoschweiz.admin.ch/service-und-publikationen/applikationen/ext/daten-ohne-programmier-kenntnisse-herunterladen.html#lang=de&mdt=normal&pgid=&sid=&col=&di=&tr=&hdr=) is mentioned.

Table 7 Generated mean power of different samples, when putting a black paper directly on the respective sample (control measurements, Figure 6).

Date	Sample	Time	global radiation averaged over ten minutes [W/m^2]	Mean Power [uW]
18.07.2025	Fabric 5	1.20-1.45pm	850	0.03±0
18.07.2025	Fabric 6	1.20-1.45pm	833	0.04±0
18.07.2025	Fabric 9	1.20-1.45pm	833	0.6±0.3

Table 8 Generated mean power during direct sun with Textal PGS on PES. Values containing the star (*) were measured during diffuse radiation. Fabric 5 (Table 3)

Date	Time	global radiation averaged over ten minutes [W/m^2]	Mean power output [uW]	Power output density [W/m^2]
03.07.2025	09.50-10.30am	808	0.8±0.1	0.01
04.07.2025	02.10-03.10pm	758	14±0.1	0.11
11.07.2025	10.00-10.30am	659	1±0	0.01
17.07.2025	08.50-09.15am	473	1.9±0	0.02
17.07.2025	02.50-03.40pm	769	20±0.1	0.16
17.07.2025	04.30-04.45pm	421	3.3±0	0.03
18.07.2025	01.20-01.45pm	833	15±0.1	0.12
18.07.2025		511 (indoor)	0.2±0	0.00
23.07.2025	09.25-10.05am	407	11±0.3	0.09
04.07.2025*	2.30-2.55pm	669*	0.8±0.0*	0.01*
11.07.2025*	9.17-10am	698*	0.9±0.2*	0.01*
11.07.2025*	4.00-4.20pm	420*	2.9±1.0*	0.03*

Table 9 Generated mean power during direct sun with Textal PGS as bottom layer on PES. A LSC made of Plextol DV 455 and 0.2wt% BY40 as dye was put on top manually. Values containing the star (*) were measured during diffuse radiation. Fabric 7 (Table 3).

Date	Time	global radiation averaged over ten minutes [W/m^2]	Power output, total [uW]	Power output density [W/m^2]	Power output from LSC [uW]
03.07.2025	09.50-10.30am	808	22±0.2	0.16	22±0.2
04.07.2025	02.10-03.10pm	758	52±0.6	0.38	38±0.6
11.07.2025	10.00-10.30am	640	35±1.6	0.26	34±1.6
17.07.2025	08.50-09.15am	473	27±0.5	0.2	25±0.5
17.07.2025	02.50-03.40pm	769	67±0.8	0.5	47±0.8
17.07.2025	04.30-04.45pm	410	48±1.0	0.35	45±1.0
18.07.2025	01.20-01.45pm	833	58±1.1	0.42	42±1.4
18.07.2025		511 (indoor)	3.5±0.1	0.03	3.4±0.1
23.07.2025	09.25-10.05am	407	33±0.4	0.24	23±0.4
04.07.2025*	2.30-2.55pm	646*	23±9.1*	0.17*	23±9.1*
11.07.2025*	9.17-10am	698*	14±1.9*	0.10*	14±1.9*
11.07.2025*	4.00-4.20pm	420*	34±7.7*	0.25*	31±7.7*

Table 10 Generated mean power during direct sun with Textal PGS as bottom layer on PES, which contained numerous air bubbles. A LSC made of Plextol DV 455 and 0.2wt% BY40 as dye was directly coated on top. Values containing the star (*) were measured during diffuse radiation. Fabric 6 (Table 3).

Date	Time	global radiation averaged over ten minutes [W/m^2]	Mean power output [uW]	Power output density [W/m^2]
03.07.2025	09.50-10.30am	808	6.9±0.1	0.06
04.07.2025	02.10-03.10pm	758	12±0.1	0.10
11.07.2025	10.00-10.30am	882	6.7±0.1	0.05
17.07.2025	08.50-09.15am	473	3.6±0.1	0.03
17.07.2025	02.50-03.40pm	769	14±2.5	0.11

17.07.2025	04.30-04.45pm	410	12±0.2	0.10
18.07.2025	01.20-01.45pm	833	7.1±0.2	0.06
18.07.2025		511 (indoor)	0.8±0.0	0.01
23.07.2025	09.25-10.05am	407	8.7±0.1	0.07
04.07.2025*	2.30-2.55pm	669*	10±0.7*	0.08*
11.07.2025*	9.17-10am	698*	2.7±0.3*	0.02*
11.07.2025*	4.00-4.20pm	420*	6.2±1.4*	0.05*

Table 7 shows, that barely any power is generated with the in-house set-up (Figure 6) through the solar cells alone. This proves that there are no big slits, where light is hitting the solar cells directly. Table 8 depicts the mean power generated by the bottom layer alone, without an LSC. These values are generated due to the textile under the guiding layer working as a scattering surface, promoting incoupling of light that would have been lost. Indeed, the addition of a scattering/reflection layer is a standard method used to improve the optical efficiency of LSCs in buildings. In our case, the textile itself completes this function. The values in the last column from Table 9 were subtracted from Table 8, to receive the output power, which is solely generated by the luminescent layer in the LSC.
For the values in Table 10, no measurement for the bottom layer alone as a reference was performed, as a result of the numerous unevenly distributed air bubbles in that layer, which complicates finding a sample in which the air bubbles are distributed in the same uneven way. However, when comparing the values in Table 9 (fabric 7) with values in Table 10 (fabric 6), the yielded power with fabric 6, containing an LSC layer, is nearly similarly low when using solely a thinner Textal layer with barely any air bubbles and no LSC layer (Fabric 5) (Table 8). Even though fabric 6 has a higher thickness compared to fabric 7, which usually has a beneficial effect on light guiding, reducing the air bubbles as much as possible has a high impact on enhancing the power output, as it prevents light from being scattered by air bubbles.

Table 11 Generated mean power during direct sun with Tubcosil HAB 5-1 on PES. Values containing the star (*) were measured during diffuse radiation. Fabric 8 (Table 3).

Date	Time	global radiation averaged over ten minutes [W/m^2]	Mean power output [uW]	Power output density [W/m^2]
11.07.2025	10.00-10.30am	659	1470±56	3.8
17.07.2025	08.50-09.15am	229	1240±14	3.2
17.07.2025	02.50-03.40pm	366	1150 ±380	3.0
17.07.2025	04.30-04.45pm	410	1880±60	4.9
18.07.2025	01.20-01.45pm	813	2070±47	5.4
18.07.2025		511 (indoor)	318±15	0.83
23.07.2025	09.25-10.05am	739	1790±19	4.7
11.07.2025*	4.00-4.20pm	385*	1500±136*	4

Table 12 Generated mean power during direct sun with Tubcosil HAB 5-1 as bottom layer on PES. A LSC made of Plextol DV 455 and 0.2wt% BY40 as dye was put on top manually. Values containing the star (*) were measured during diffuse radiation. Fabric 9 (Table 3).

Date	Time	global radiation averaged over ten minutes [W/m^2]	Power output, total [uW]	Power output density [W/m^2]	Power output from LSC [uW]
03.07.2025	09.50-10.30am	852	1130±16	2.7	No reference
04.07.2025	02.10-03.10pm	758	1980±34	4.8	No reference
11.07.2025	10.00-10.30am	659	2020±1.1	4.9	554±1.1
17.07.2025	08.50-09.15am	229	1440±9.9	3.5	206±9.9
17.07.2025	02.50-03.40pm	366	2350±46	5.7	1200±46

17.07.2025	04.30-04.45pm	410	1920±10	4.6	42±10
18.07.2025	01.20-01.45pm	813	2170±26	5.2	99±26
18.07.2025		511 (indoor)	355±20	0.85	36±20
23.07.2025	09.25-10.05am	664	1790±2.1	4.3	Not meaningful
04.07.2025*	2.30-2.55pm	717*	622±41*	1.5	No reference*
11.07.2025*	9.17-10am	640*	1532±46*	4	No reference*
11.07.2025*	4.00-4.20pm	385*	2035±15*	5	535±15*

Table 13 Generated mean power during direct sun with Tubcosil HAB 5-1 on PES. The value containing the star (*) was measured during diffuse radiation. Fabric 10 (Table 3).

Date	Time	global radiation averaged over ten minutes [W/m^2]	Mean power output [uW]	Power output density [W/m^2]
03.07.2025	09.50-10.30am	808	3.8±0.0	0.04
04.07.2025	02.10-03.10pm	758	29±0.0	0.29
11.07.2025	10.00-10.30am	640	3.4±0.1	0.03
17.07.2025	08.50-09.15am	229	10±0.1	0.10
17.07.2025	02.50-03.40pm	769	7.7±0.2	0.08
17.07.2025	04.30-04.45pm	410	6±0.2	0.06
18.07.2025	01.20-01.45pm	833	19±0.7	0.19
18.07.2025		511 (indoor)	0.5±0.1	0.00
23.07.2025	09.25-10.05am	295	12±0.1	0.12
04.07.2025*	2.30-2.55pm	686*	21±6.3*	0.21*
11.07.2025*	9.17-10am	640*	13±0.3*	0.3*
11.07.2025*	4.00-4.20pm	385*	1.2±0.1*	0.01*

Table 14 Generated mean power during direct sun with Tubcosil HAB 5-1 as bottom layer on PES. A LSC made of Plextol DV 455 and 0.2wt% BY40 as dye was put on top manually. Values containing the star (*) were measured during diffuse radiation. Fabric 11 (Table 3).

Date	Time	global radiation averaged over ten minutes [W/m^2]	Power output, total [uW]	Power output density [W/m^2]	Power output from LSC [uW]
11.07.2025	10.00-10.30am	970	19±0.2	0.17	16±0.2
17.07.2025	08.50-09.15am	229	11±0.1	0.10	0.9±0.1
17.07.2025	02.50-03.40pm	656	8.7±0.1	0.08	1±0.1
17.07.2025	04.30-04.45pm	410	6±0.1	0.06	0.±0.1
18.07.2025	01.20-01.45pm	813	10±0.3	0.09	Not meaningful
18.07.2025		511 (indoor)	0.5±0	0.00	0±0
23.07.2025	09.25-10.05am	295	4.7±0.1	0.04	Not meaningful
11.07.2025*	9.17-10am	640*	4±0.2*	0.04*	Not meaningful*
11.07.2025*	4.00-4.20pm	385*	3.6±0.8*	0.03*	2.4±0.8*

The increase in generated power is around 40 times higher when increasing the thickness by a factor of four only (Table 13 and Table 11). Comparing fabric 8 (Table 11) with fabric 9 (Table 12) shows that adding an LSC layer (Table 12) leads to an enhanced power output. However, when looking closer at the data in Table 12 the energy output seems to decrease with each measurement. A possible explanation could be that with each additional measurement the LSC layer was removed (page 10), leading to more dirt accumulation on the PDMS bottom layer and therefore, to a decline in power gen-

eration. Furthermore, with every subsequent measurement, there was the possibility of increased mechanical mismatch between the LSC layer and the guiding layer, leading to a rise in optical losses. The comparison of fabric 5 (Table 8) with fabric 10 (Table 13) indicates that the degree of light guiding in the respective polymers is roughly the same, considering that fabric 5 (Table 2) is slightly thinner than fabric 10 (Table 3). The advantage of using Textal PGS as bottom layer is, that it allows the direct application of the LSC layer made of Plextol DV 455. Therefore, although the non-covalent attachment (fabric 10 and fabric 11) presents advantages in terms of ease of fabrication and potential for recyclability (easier end-of-life), the homogenous/covalent application of the LSC layer presents clear advantages in terms of optical power and light coupling. Despite being challenging in fabrication, it should be selected due to these properties.

Table 15 Generated mean power during direct sun with Plextol DV 455 on PES. Values containing the star (*) were measured during diffuse radiation. Fabric 12 (Table 3).

Date	Time	global radiation averaged over ten minutes [W/m^2]	Mean power output [uW]	Power output density [W/m^2]
03.07.2025	09.50-10.30am	852	0±0	0
04.07.2025	02.10-03.10pm	717	0.1±0	0
11.07.2025	10.00-10.30am	659	0±0	0
17.07.2025	08.50-09.15am	379	0±0	0
17.07.2025	02.50-03.40pm	366	3.6±0.1	0.02
17.07.2025	04.30-04.45pm	410	0±0	0
18.07.2025	01.20-01.45pm	813	0±0	0
18.07.2025		511 (indoor)	0±0	0
23.07.2025	09.25-10.05am	664	0±0	0
04.07.2025*	2.30-2.55pm	686*	3.4±3.5*	0.02*
11.07.2025*	9.17-10am	649*	0.02±0*	0*
11.07.2025*	4.00-4.20pm	174*	0.03±0.01*	0*

Table 16 Generated mean power during direct sun with Plextol DV 455 as bottom layer on PES. A LSC made of Plextol DV 455 and 0.2wt% BY40 as dye was put on top manually. Values containing the star (*) were measured during diffuse radiation. Fabric 13 (Table 3).

Date	Time	global radiation averaged over ten minutes [W/m^2]	Power output, total [uW]	Power output density [W/m^2]	Power output from LSC [uW]
03.07.2025	09.50-10.30am	852	14±0.1	0.08	14±0.1
04.07.2025	02.10-03.10pm	717	20±0.1	0.11	20±0.01
11.07.2025	10.00-10.30am	659	11±0.2	0.06	11±0.2
17.07.2025	08.50-09.15am	379	9.4±0.6	0.05	9.4±0.6
17.07.2025	02.50-03.40pm	366	111±2.1	0.60	107±2.1
17.07.2025	04.30-04.45pm	410	9.4±2.1	0.05	9.4±2.1
18.07.2025	01.20-01.45pm	813	149±2	0.81	149±2
18.07.2025		511 (indoor)	0.7±0.1	0.00	0.73±0.1
23.07.2025	09.25-10.05am	664	101±0.7	0.55	101±0.7
04.07.2025*	2.30-2.55pm	669*	12±5.7*	0.07*	9.1±5.7*
11.07.2025*	9.17-10am	649*	6.6±0.9*	0.04*	6.6±0.9*
11.07.2025*	4.00-4.20pm	174*	11±2.6*	0.06*	11±2.6*

Table 17 Generated mean power during direct sun with Plextol DV 455 on PES. Values containing the star (*) were measured during diffuse radiation. Fabric 14 (Table 3).

Date	Time	global radiation averaged over ten minutes [W/m^2]	Mean power output [uW]	Power output density [W/m^2]
03.07.2025	09.50-10.30am	852	1.8±0.0	0.01
04.07.2025	02.10-03.10pm	618	81±0.4	0.36
11.07.2025	10.00-10.30am	970	53±2.4	0.24
17.07.2025	08.50-09.15am	379	1.1±0.0	0.00
17.07.2025	02.50-03.40pm	366	139±1.3	0.62
17.07.2025	04.30-04.45pm	410	1.9±0.1	0.01
18.07.2025	01.20-01.45pm	813	180±3.6	0.80
18.07.2025		511 (indoor)	18±0.6	0.08
23.07.2025	09.25-10.05am	794	115±0.4	0.51
04.07.2025*	2.30-2.55pm	717*	1.1±0.1*	0*
11.07.2025*	9.17-10am	649*	33±3.7*	0.15*
11.07.2025*	4.00-4.20pm	174*	0.7±0.2*	0*

Table 18 Generated mean power during direct sun with Plextol DV 455 as bottom layer on PES. A LSC made of Plextol DV 455 and 0.2wt% BY40 as dye was put on top manually. Values containing the star (*) were measured during diffuse radiation. Fabric 15 (Table 3).

Date	Time	global radiation averaged over ten minutes [W/m^2]	Power out-put, total [uW]	Power out-put density [W/m^2]	Power output from LSC [uW]
03.07.2025	09.50-10.30am	491	147±0.5	0.62	145±0.5
04.07.2025	02.10-03.10pm	618	245±1.6	1.03	164±1.6
11.07.2025	10.00-10.30am	774	222±25	0.94	170±25
17.07.2025	08.50-09.15am	379	171±1.4	0.72	170±1.4
17.07.2025	02.50-03.40pm	366	252±2.2	1.06	113±2.2
17.07.2025	04.30-04.45pm	410	262±9.8	1.10	261±9.8
18.07.2025	01.20-01.45pm	813	75±2.0	0.32	Not meaning-ful
18.07.2025		511 (indoor)	33±0.6	0.14	15±0.6
23.07.2025	09.25-10.05am	794	35±0.4	0.15	Not meaning-ful
04.07.2025*	2.30-2.55pm	717*	22±15*	0.09*	21±15*
11.07.2025*	9.17-10am	649*	89±5.4*	0.38*	56±5.4*
11.07.2025*	4.00-4.20pm	174*	134±80*	0.57*	134±80*

When comparing fabric 7 (Table 9) with fabric 13 (Table 16), the generated power was higher for fabric 7, when taking the lower thickness (Table 3) of fabric 7 in consideration. An increase in thickness of 0.5mm (50%) resulted in approximately three times more power generation (

04.07.2025*	2.30-2.55pm	717*	1.1±0.1*	0*
11.07.2025*	9.17-10am	649*	33±3.7*	0.15*
11.07.2025*	4.00-4.20pm	174*	0.7±0.2*	0*

Table 18 and Table 16). Taking everything in consideration and when the bottom layer should have a thickness around 1mm, fabric 7 showed the most promising results.
All indoor measurements of the respective samples (Table 8 to

04.07.2025*	2.30-2.55pm	717*	1.1±0.1*	0*
11.07.2025*	9.17-10am	649*	33±3.7*	0.15*
11.07.2025*	4.00-4.20pm	174*	0.7±0.2*	0*

Table 18) showed low power outputs than the same sample under the sun with a similar irradiance. While the power output gives information about how much energy is arriving, solar cells respond to photon flux as well. Through the indoor lamp, the number of useable photons is lower, as the light source does not cover the whole solar spectrum. The lower the photon flux, the less electrons are generated, resulting in a lower current. This explains why the current measured under indoor lightning was lower than under outdoor conditions, resulting in a reduced power output. However, a measuarable power output was still detected in all cases.

For Textal, the generated power from diffuse radiation was comparable to the output from direct sunlight. This was observed as well with Tubcosil and when applying a thinner layer of Plextol DV 455. When using a thicker layer of Plextol in combination with a LSC layer, a lower energy output was observed (

04.07.2025*	2.30-2.55pm	717*	1.1±0.1*	0*
11.07.2025*	9.17-10am	649*	33±3.7*	0.15*
11.07.2025*	4.00-4.20pm	174*	0.7±0.2*	0*

Table 18). In general, we can infer that the textile LSCs work independently of the solar energy being direct or diffuse, which is also a known advantage of standard LSCs and would justify their use under variable irradiation conditions.

3 Conclusions and outlook

Conclusions

LSCs based on acrylate waterborne polymers are very promising candidates for film-based LSCs, due to the good transparency of the host material and their water-based nature. We showed that different curing processes were applied- polymerization through water evaporation or through UV-curing. Leakage tests have shown that only maximum amounts of 0.025wt% of the incorporated dye are released. Some of the chosen polymers showed surface changes after exposure to water, while others present high surface stickiness, what is a drawback for the intended application. Therefore, due to the higher transparency and therefore better light transmission, LSCs for WP3 were mainly made of Plextol DV 455 containing 0.02wt% BY40 for subsequent experiments. For fiber-based LSCs, acrylate and APCN are ideal polymers, while LR305 and coumarin 6 are the best dyes.

Urethane-based resins are also suited for LSCs due to their high transmittance in the visible region and lower price as compared to acrylate and siloxane resins, besides being partially bio-based. However, its pot life is too short, making it difficult to prepare large-area pieces.

Two fabrication methods – molding and microfluidic wet-spinning (MWS) – were used to obtain LSC fibers. With MWS, the generation of acrylate or APCN fibers was enabled, therefore allowing the incorporation of hydrophobic and hydrophilic luminophores in the same host matrix. This is an advantage as the fluorophore is then not restricted to the hydrophobicity of the luminophore anymore. Reproducible spinning of 90 to 210cm long APCN fibers was achieved. However, due to Schoeller's focus on coated textiles, we decided to fully concentrate the development on film-based LSC. Therefore, for WP4 & WP5, no fiber-based LSC was developed.

We demonstrated the production of film-based LSCs based on polymers and dyes selected in WP1. We also established that only double-layer LSC films are interesting for the proposed application. We focused on fabricating double-layer LSCs with commercially available polymers used in the textile industry as our bottom layer. Several of the transparent textile coatings presented drawback and were not further considered (tendency to penetrate the fabric instead of forming a film on its surface, leakage, too high stickeness, etc.). Therefore, only the following materials were chosen for WP4 & WP5: Textal PGS (urethane, Textilcolor AG), Tubcosil HAB 5-1 (siloxane, CHT Germany GmbH), and the aqueous emulsion of a self-crosslinking acrylic polymer Plextol 455 (acrylate, Synthomer). For the upper layer Plextol DV 455 was used. The upper LSC layer contained 0.2wt% BY40. These LSCs can be easily scaled up, as the individual components (polymer and dye) already find application in the textile industry.

At Schoeller water vapor permeation (EN ISO 11092) was tested for the samples containing Textal PGS as bottom layer on polyester (PES), which was around zero. Washing tests according to EN ISO 105-C06 indicated no detachment of fabrics coated with Textal PGS. The above-mentioned experiments with the LSC layer attached to the Textal PGS were not possible to conduct due to the liquidation of Schoeller in Sevelen this summer.

Unfortunately, due to the delivery stop of flexible PSCs from Saule Technologies, there were not enough solar cells to be integrated in a textile for a proof of concept/demonstrator. As mentioned in the text, this was due to the imminent bankruptcy of the company. We could not find any alternative company that can produce modules small and flexible enough to be integrated into the textiles.

Samples containing Textal PGS, Tubcosil HAB 5-1, and Plextol 455 were coated on a PES. On top of those polymeric films a LSC layer made of Plextol DV 455 was either directly coated on top or separately fabricated and then manually applied. Depending on the system, the samples demonstrated promising power outputs ranging from the tens to hundreds of microwatts. Considering the fabrication process, the power output, and by choosing a bottom layer, with a thickness of around 1mm, the material of choice would be Textal PGS (fabric 7) as the bottom layer. Due to the delivery stop of flexible PSCs from Saule Technologies, no demonstrator was built as we were notified at too short notice. The initial idea was to fabricate six squares containing Textal PGS as bottom layer and Plextol DV 455 with 0.2wt% BY40 as LSC layer (fabric 7, Table 3). Each square would have dimensions of about 10x10cm^2. These would be sewn to the back of a jacket. At the edges, the flexible PSCs from Saule Technologies should be mounted, 2 per edge, totalling 8 SC modules per unit. According to our results in WP5, such a construction would be able to deliver about 65 uW per edge, or 265 uW per unit (**1.6 mW** for the 6 units, (**0.5 W/m^2** when considering the effective solar cell area). An alternative design would be to use thicker, smaller LSC units (5x5cm^2, 3.5 mm thickness, fabric 9, Table 12), which could deliver (according to our results) 4.6 mW per unit and **28 mW** in total (**5.7 W/m^2** when considering the effective solar cell area).

Outlook

PSCs show very promising results due to their excellent absorption in the visible spectrum of light and its cell's external quantum efficiency (ECE) is high at the emission wavelength of the dye BY40, which is crucial to efficiently harvest the luminescent emission. The SC we acquired (From Saule Technologies) had, however, low PCE and power generation. According to the datasheet, they only generate 0.18 W/m^2 under 500 lx, which would correspond to about 36 W/m^2 under direct sunlight (~1000 W/m^2)! This limited the power output that could be obtained with our textile LSC units but, despite this, were still the best choice for building the demonstrator. We could not find any other supplier of small, flexible, high PCE SC that could be integrated with our fabrics.
Despite these shortcomings, the results obtained in WP5 are promising enough to continue the development of wearable LSCs. Given the closing of Schoeller, we will in the following months, contact other textile specialist companies to continue the project. One potential partner would be CHT, with whom we informally collaborated and provided us with alternative polymers that were used in the project. The focus would be on improving the light coupling between both layers (LSC and guiding layer) as well as to the SC modules.
Moreover, we will continue searching for small and flexible SC modules. Potentially interesting suppliers include Sunplugged's solarfoil (Austria), Midsummer (Sweden), Enfoil (Belgium), and Ascent Solar (US).

4 Publications and other communications

- Article from Radio SRF 3. "Strom der Zukunft- Smartphone mit der Jacke laden"

Link: Strom der Zukunft - Smartphone mit der Jacke laden - Radio SRF 3 - SRF

- TV report by SRF news for the show "10vor10" as highlight report under the topic "Die Idee".

Link

https://www.srf.ch/play/tv/10-vor-10/video/10-vor-10-vom-23-08-2024?urn=urn:srf:video:d85f356d-b271-4bbc-ae74-d56ccb337ed0

https://www.youtube.com/watch?v=_G2k2zR4ZJA

- Presentation in the Biannual meeting of the Subitex Initiative (11.03.24): "Wearable Luminescent Solar Concentrators"
- Invited Presentation at the Annual Meeting of Swiss Textiles Innovation Day 2024 – Special Edition (06.11.24). "Wearable Luminescent Solar Concentrators"

Link: https://swisstextiles.ch/veranstaltungen/innovation-day-2024-150-years-of-impact

- Presentation at the "Materials Today Conference 2025" (23.7.2025): "Designing Amphiphilic Polymer Conetworks for application as wearbale luminescent solar concentrator"
- Interview for the SNF Horizonte magazine (will appear in the September/25 issue).

5 References

[1] S. A. Hashemi, S. Ramakrishna, und A. G. Aberle, „Recent progress in flexible–wearable solar cells for self-powered electronic devices“, *Energy Env. Sci*, Bd. 13, Nr. 3, S. 685–743, 2020, doi: 10.1039/C9EE03046H.

[2] R. Liu, Z. L. Wang, K. Fukuda, und T. Someya, „Flexible self-charging power sources“, *Nat. Rev. Mater.*, Bd. 7, Nr. 11, S. 870–886, Nov. 2022, doi: 10.1038/s41578-022-00441-0.

[3] F. Meinardi, F. Bruni, und S. Brovelli, „Luminescent solar concentrators for building-integrated photovoltaics“, *Nat. Rev. Mater.*, Bd. 2, Nr. 12, S. 17072, Nov. 2017, doi: 10.1038/natrevmats.2017.72.

[4] J. Roncali, „Luminescent Solar Collectors: Quo Vadis?“, *Adv. Energy Mater.*, Bd. 10, Nr. 36, S. 2001907, 2020, doi: https://doi.org/10.1002/aenm.202001907.

[5] I. Papakonstantinou, M. Portnoi, und M. G. Debije, „The Hidden Potential of Luminescent Solar Concentrators“, *Adv. Energy Mater.*, Bd. 11, Nr. 3, S. 2002883, 2021, doi: https://doi.org/10.1002/aenm.202002883.

[6] P. Minei, G. Iasilli, G. Ruggeri, und A. Pucci, „Luminescent Solar Concentrators from Waterborne Polymer Coatings“, *Coatings*, Bd. 10, Nr. 7, 2020, doi: 10.3390/coatings10070655.

[7] A. Gursoy *u. a.*, „Facile Fabrication of Microfluidic Chips for 3D Hydrodynamic Focusing and Wet Spinning of Polymeric Fibers“, *Polymers*, Bd. 12, Nr. 3, 2020, doi: 10.3390/polym12030633.

[8] M. Rother *u. a.*, „Self-Sealing and Puncture Resistant Breathable Membranes for Water-Evaporation Applications“, *Adv. Mater.*, Bd. 27, Nr. 42, S. 6620–6624, 2015, doi: https://doi.org/10.1002/adma.201502761.

[9] R. Barciela *u. a.*, „Monte Carlo simulation of a LSC based on stacked layers of fiber arrays with core-coating different absorbing properties“, *Opt Express*, Bd. 29, Nr. 13, S. 19566–19585, Juni 2021, doi: 10.1364/OE.422694.

[10] W. Raja *u. a.*, „Photon recycling in perovskite solar cells and its impact on device design“, Bd. 10, Nr. 8, S. 2023–2042, 2020, doi: 10.1515/nanoph-2021-0067.

[11] A. Galliano, S. Bistac, und J. Schultz, „Adhesion and friction of PDMS networks: molecular weight effects“, *J. Colloid Interface Sci.*, Bd. 265, Nr. 2, S. 372–379, Sep. 2003, doi: 10.1016/S0021-9797(03)00458-2.

[12] M. Gratzel und P. Liska, „Photo-electrochemical cell“, 4,927,721, 22. Mai 1990

[13] M. Islam, N. Kassim, A. Alkahtani, und N. Amin, „Assessing the Impact of Spectral Irradiance on the Performance of Different Photovoltaic Technologies“, 2021. doi: 10.5772/intechopen.96697.

[14] H. Ahmed, S. J. McCormack, und J. Doran, „External Quantum Efficiency Improvement with Luminescent Downshifting Layers: Experimental and Modelling“, *Int. J. Spectrosc.*, Bd. 2016, Nr. 1, S. 8543475, Jan. 2016, doi: 10.1155/2016/8543475.